Published OnlineFirst June 6, 2012; DOI: 10.1158/1078-0432.CCR-12-0073

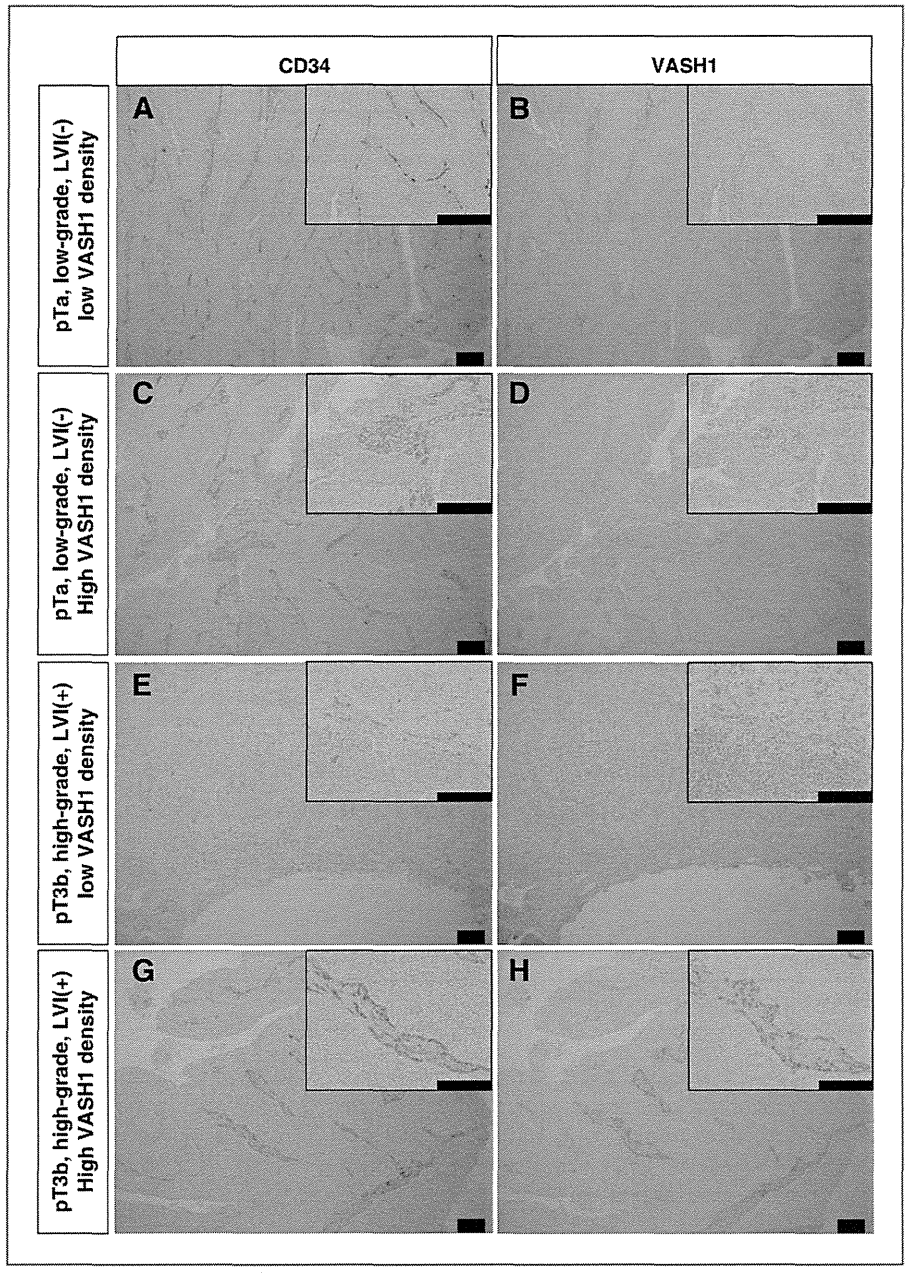

Figure 1. Immunostaining for CD34 (A, C, E, and G) and VASH1 (B, D, F, and H) in the same case of UTUC. pTa, low-grade, and LVI-negative UTUC with low VASH1 density (A and B) or high VASH1 density (C and D). pT3b, high-grade, and LVI-positive UTUC with low VASH1 density (E and F) or high VASH1 density (G and H). Bar, 0.2 mm.

(10.6–44.4 for recurrence-free survival, 12.7–65.0 for cancer-specific survival). According to the risk stratification for UTUC based on prognostic factors, 31 patients (18.1%) were in the low-risk group (low tumor grade, LVI negative, and low VASH1 density), 31 patients (18.1%) in the high-risk group (any tumor grade, LVI positive, and high VASH1 density) and 109 patients (63.8%) in the intermediate-risk group (all others). The 5-year recurrence-free survival and cancer-specific survival rates were 96.4% and 96.4% in the low-risk group, 79.0% and 85.1% in the intermediate-risk group, and 30.7% and 41.3% in the high-risk group, respectively. The differences among the groups were significant ($P = 0.015$ in recurrence-free survival and $P = 0.027$ in cancer-specific survival for low- vs. intermediate-risk group, $P < 0.001$ for low- vs. high-risk group and $P < 0.001$ for intermediate- vs. high-risk group in recurrence-free survival and cancer-specific survival).

Discussion

In the present study, we retrospectively evaluated the impact of VASH1 expression by immunohistochemistry in a series of patients with locally advanced UTUC treated

Published OnlineFirst June 6, 2012; DOI: 10.1158/1078-0432.CCR-12-0073

Table 2. Univariate and multivariate analysis for recurrence-free survival and cancer-specific survival

	Recurrence-free survival			Cancer-specific survival		
		Multivariate			Multivariate	
Characteristic	Univariate *P*	HR (95% CI)	*P*	Univariate *P*	HR (95% CI)	*P*
Age, y	0.752			0.409		
<70						
≥70						
Gender	0.580			0.392		
Male						
Female						
Tumor location	0.626			0.396		
Renal pelvis						
Ureter						
Tumor grade	<0.001		0.021	<0.001		0.030
Low						
High		4.20 (1.24–14.2)			5.10 (1.16–22.3)	
Pathologic T stage	<0.001			<0.001		
<pT2						
≥pT2						
Lymphvascular invasion	<0.001		<0.001	<0.001		<0.001
Positive		5.05 (2.45–10.4)			5.72 (2.46–13.3)	
Negative						
Adjuvant chemotherapy	<0.001			0.001		
Yes						
No						
MVD	0.216			0.473		
<70/mm^2						
≥70/mm^2						
VASH1 density	0.017		0.024	0.042		0.031
<40/mm^2						
≥40/mm^2		2.10 (1.10–3.99)			2.23 (1.08–4.60)	

Abbreviation: CI, confidence interval.

in a single center. Our results suggested that VASH1 expression was a prognostic indicator in addition to other standard factors such as tumor grade and the presence of LVI. High VASH1 density was related to shorter patient survival. To the best of our knowledge, this is the first study evaluating prognostic value of VASH1 expression in patients with cancer.

Angiogenesis has a critical role in tumor growth and metastasis (11). Recent studies revealed significant roles for angiogenesis in the prediction of survival in patients with different malignancies (23, 27). One of the biomarkers that could reflect angiogenic aggressiveness was MVD (12–14). Several studies on urothelial carcinoma indicated that the status of MVD was associated with clinical outcomes, such as tumor grade and pathologic stage, and could be an independent prognostic factor of patient survival (13–15). However, to date evidence of the prognostic role of MVD in urothelial carcinoma is contradictory, suggesting the prognostic impact of MVD might be controversial (17–19). In the present study, we found no significant association between MVD or patient mortality and survival. One of the reasons might be because MVD corresponds to the number of accomplished vessels and includes vessels without the potential of neovascularization in tumors.

VASH1 has been isolated from VEGF inducible genes in endothelial cells present in newly formed blood vessels behind the sprouting front where angiogenesis terminates (28, 29). Recently, histologic evidence of VASH1 expression has been found in samples from patients with breast cancer (25), cervical carcinoma (23), and endometrial carcinoma (30). These reports indicated that VASH1 expression was associated with tumor grade and histologic type of carcinomas. Moreover, it was reported that VASH1 expression tended to be concordant with MVD although partial dissociation was observed in some patients with breast carcinoma. VASH1 expression was significantly higher in invasive breast carcinoma, although no significant difference was observed in the levels of MVD between patients with invasive disease or not. They also suggested that an evaluation of the number of VASH1-

Published OnlineFirst June 6, 2012; DOI: 10.1158/1078-0432.CCR-12-0073

Table 3. Clinicopathologic parameters in 171 patients according to the level of the VASH1 density

Characteristic	No of patients (%)		P
	Patients with VASH1 density <40/mm^2	Patients with VASH1 density ≥40/mm^2	
No of patients	88	83	
Age, y			0.744
<70	52 (59.1)	47 (56.6)	
≥70	36 (40.9)	36 (43.4)	
Gender			0.347
Male	71 (80.7)	62 (74.7)	
Female	17 (19.3)	21 (25.3)	
Tumor location			0.893
Renal pelvis	52 (59.1)	49 (59.0)	
Ureter	36 (40.9)	34 (41.0)	
Tumor grade			0.044
Low	35 (39.8)	21 (25.3)	
High	53 (60.2)	62 (74.7)	
Pathologic T stage			0.001
<pT2	44 (50.0)	21 (25.3)	
≥pT2	44 (50.0)	62 (74.7)	
Lymphvascular invasion			0.773
Positive	31 (35.2)	31 (37.3)	
Negative	57 (64.8)	52 (62.7)	
Adjuvant chemotherapy			0.159
Yes	11 (12.5)	17 (20.5)	
No	77 (87.5)	66 (79.5)	
MVD			<0.001
<70/mm^2	65 (73.9)	25 (30.1)	
≥70/mm^2	23 (26.1)	58 (69.9)	

positive vessels may become one of the prognostic biomarkers for metastasis and prognosis (26). These results indicate that VASH1 could become a new molecular biomarker, which influences angiogenic heterogeneity of tumors.

Our study showed that UTUC with a higher number of VASH1-positive vessels tended to have a poor prognosis. We found a significant correlation among VASH1 density, tumor grade, and pathologic T stage. In multivariate analysis, high VASH1 density was an independent

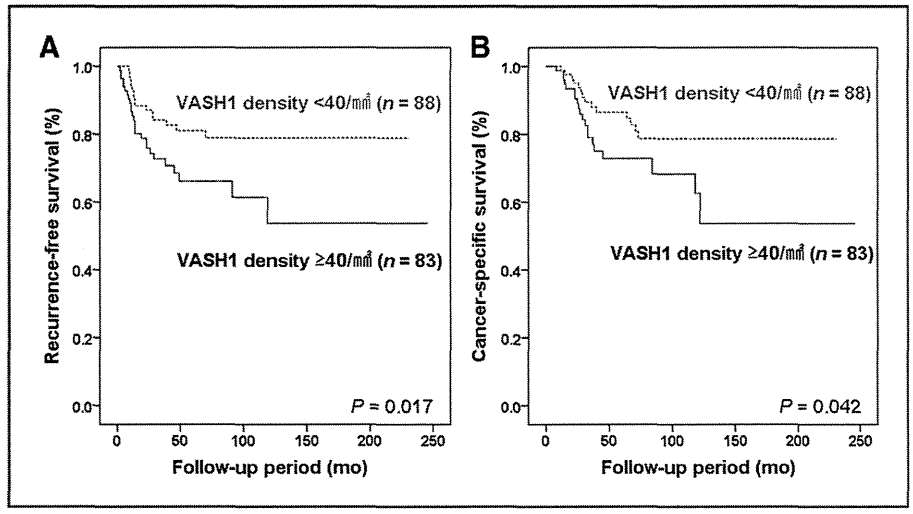

Figure 2. Kaplan–Meier recurrence-free survival (A) and cancer-specific survival (B) of the patients after surgery for UTUC according to VASH1 density.

Published OnlineFirst June 6, 2012; DOI: 10.1158/1078-0432.CCR-12-0073

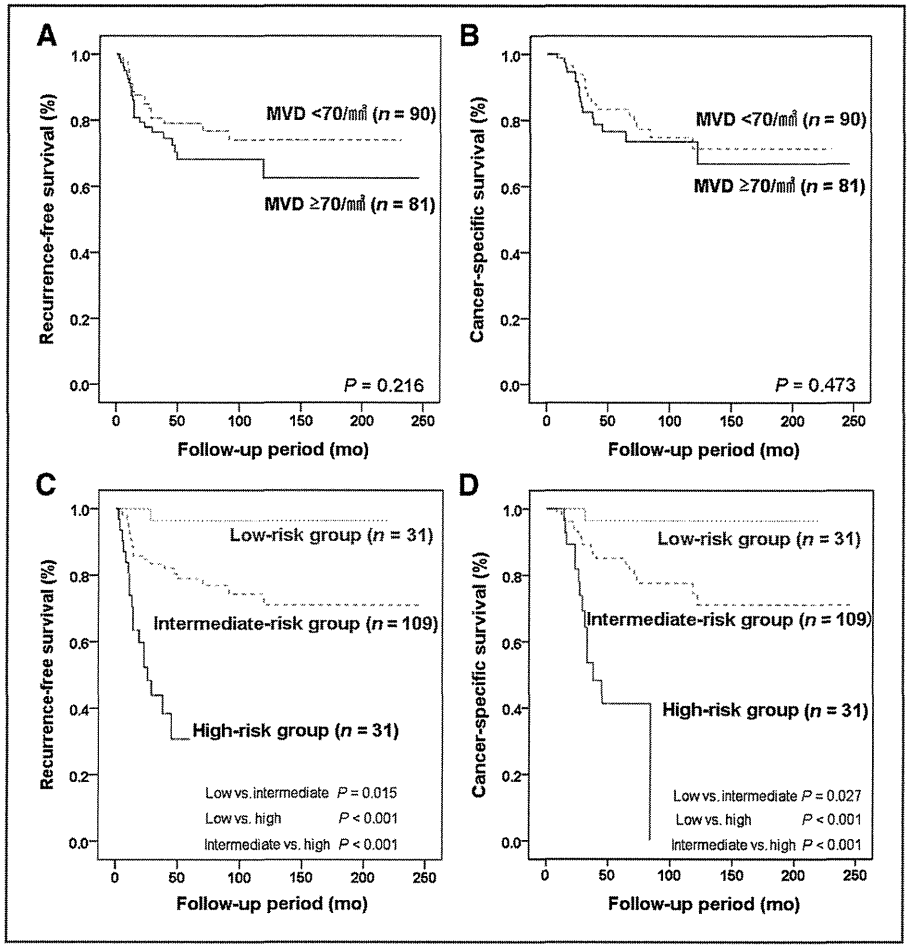

Figure 3. Kaplan–Meier recurrence-free survival (A) and cancer-specific survival (B) of the patients after surgery for UTUC according to MVD. Kaplan–Meier curves of recurrence-free survival (C) and cancer-specific survival (D) of the patients after surgery for UTUC according to tumor grade, LVI, and VASH1 density stratified according to 3 risk groups. Low-risk group consisted of patients with low-grade tumor, LVI-negative, and low VASH1 density. High-risk group consisted of those with any tumor grade, LVI-positive, and high VASH1 density. All others were included in the intermediate-risk group.

prognostic factor, suggesting the status of VASH1 density could serve as a biomarker of the malignant potential of tumor angiogenesis. These results suggest that the level of VASH1 expression may influence the clinical course of a disease.

Using VASH1 density and other independent indicators, we established a prognostic risk stratification for UTUC. Patients were stratified into 3 groups according to statistical modeling based on the relative risk associated with the prognostic indicators derived from multivariate analysis. As shown in Fig. 3C and D among patients with UTUC, the patients with positive LVI and higher VASH1 density showed a worse prognosis than other groups ($P < 0.001$). This stratification made it possible to have a more accurate survival prediction, suggesting more appropriate follow-up including computerized tomography and the timing for aggressive treatments such as chemotherapy.

This study has several limitations. First, it was conducted in a retrospective manner and in a limited number of patients. Not all patients received adjuvant chemotherapy, which may have had an effect on subsequent tumor progression. Thus, a prospective study in a large population is warranted to clarify the prognostic role of VASH1 expression in UTUC.

Disclosure of Potential Conflicts of Interest

No potential conflicts of interest were disclosed.

Authors' Contributions

Conception and design: Y. Miyazaki, T. Kosaka, E. Kikuchi, N. Tanaka, Y. Sato, M. Oya
Development of methodology: N. Tanaka, M. Oya
Acquisition of data (provided animals, acquired and managed patients, provided facilities, etc.): Y. Miyazaki, T. Kosaka, S. Mikami, N. Tanaka, T. Maeda, M. Ishida, M. Oya
Analysis and interpretation of data (e.g., statistical analysis, biostatistics, computational analysis): Y. Miyazaki, T. Kosaka, S. Mikami, N. Tanaka, M. Ishida, M. Oya
Writing, review, and/or revision of the manuscript: Y. Miyazaki, T. Kosaka, S. Mikami, E. Kikuchi, N. Tanaka, A. Miyajima, K. Nakagawa, Y. Okada, Y. Sato, M. Oya
Administrative, technical, or material support (i.e., reporting or organizing data, constructing databases): Y. Miyazaki, T. Kosaka, N. Tanaka, A. Miyajima, K. Nakagawa, Y. Okada, M. Oya
Study supervision: E. Kikuchi, N. Tanaka, K. Nakagawa, M. Oya

Acknowledgments

The authors thank colleagues from the Department of Vascular Biology, Institute of Development, Aging, and Cancer, Tohoku University for their excellent technical assistance in purifying anti-human VASH1 mAb.

Published OnlineFirst June 6, 2012; DOI: 10.1158/1078-0432.CCR-12-0073

Grant Support

This work was supported by a Keio University Grant-in-Aid for Encouragement of Young Medical Scientists and the Cooperative Research Project Program of Joint Usage/Research Center at the Institute of Development, Aging and Cancer, Tohoku University.

The costs of publication of this article were defrayed in part by the payment of page charges. This article must therefore be hereby marked *advertisement* in accordance with 18 U.S.C. Section 1734 solely to indicate this fact.

Received January 9, 2012; revised May 15, 2012; accepted May 16, 2012; published OnlineFirst June 6, 2012.

References

1. Oosterlinck W. Ureteral tumour: a specific upper urinary tract transitional cell carcinoma. Eur Urol 2007;51:1164–5.
2. Rouprêt M, Zigeuner R, Palou J, Boehle A, Kaasinen E, Sylvester R, et al. European guidelines for the diagnosis and management of upper urinary tract urothelial cell carcinomas: 2011 update. Eur Urol 2011;59:584–94.
3. Kikuchi E, Horiguchi Y, Nakashima J, Hatakeyama N, Matsumoto M, Nishiyama T, et al. Lymphovascular invasion independently predicts increased disease specific survival in patients with transitional cell carcinoma of the upper urinary tract. J Urol 2005;174:2120–3.
4. Ishida M, Mikami S, Kikuchi E, Kosaka T, Miyajima A, Nakagawa K, et al. Activation of the aryl hydrocarbon receptor pathway enhances cancer cell invasion by upregulating the MMP expression and is associated with poor prognosis in upper urinary tract urothelial cancer. Carcinogenesis 2010;31:287–95.
5. Kosaka T, Kikuchi E, Mikami S, Miyajima A, Shirotake S, Ishida M, et al. Expression of snail in upper urinary tract urothelial carcinoma: prognostic significance and implications for tumor invasion. Clin Cancer Res 2010;16:5814–23.
6. Kikuchi E, Margulis V, Karakiewicz PI, Roscigno M, Mikami S, Lotan Y, et al. Lymphovascular invasion predicts clinical outcomes in patients with node-negative upper tract urothelial carcinoma. J Clin Oncol 2009;27:612–8.
7. Margulis V, Shariat SF, Matin SF, Kamat AM, Zigeuner R, Kikuchi E, et al. Outcomes of radical nephroureterectomy: a series from the Upper Tract Urothelial Carcinoma Collaboration. Cancer 2009;115:1224–33.
8. Inoue K, Kamada M, Slaton JW, Fukata S, Yoshikawa C, Tamboli P, et al. The prognostic value of angiogenesis and metastasis-related genes for progression of transitional cell carcinoma of the renal pelvis and ureter. Clin Cancer Res 2002;8:1863–70.
9. Zigeuner R, Shariat SF, Margulis V, Karakiewicz PI, Roscigno M, Weizer A, et al. Tumour necrosis is an indicator of aggressive biology in patients with urothelial carcinoma of the upper urinary tract. Eur Urol 2010;57:575–81.
10. Sato Y. Molecular diagnosis of tumor angiogenesis and anti-angiogenic cancer therapy. Int J Clin Oncol 2003;8:200–6.
11. Folkman J. Tumor angiogenesis: therapeutic implications. N Engl J Med 1971;285:1182–6.
12. Weidner N, Semple JP, Welch WR, Folkman J. Tumor angiogenesis and metastasis–correlation in invasive breast carcinoma. N Engl J Med 1991;324:1–8.
13. Bochner BH, Cote RJ, Weidner N, Groshen S, Chen SC, Skinner DG, et al. Angiogenesis in bladder cancer: relationship between microvessel density and tumor prognosis. J Natl Cancer Inst 1995;87:1603–12.
14. Shirotake S, Miyajima A, Kosaka T, Tanaka N, Maeda T, Kikuchi E, et al. Angiotensin II type 1 receptor expression and microvessel density in human bladder cancer. Urology 2011;77:1009.e19–25.
15. Inoue K, Slaton JW, Karashima T, Yoshikawa C, Shuin T, Sweeney P, et al. The prognostic value of angiogenesis factor expression for predicting recurrence and metastasis of bladder cancer after neoadjuvant chemotherapy and radical cystectomy. Clin Cancer Res 2000;6:4866–73.
16. Miyata Y, Kanda S, Nomata K, Hayashida Y, Kanetake H. Expression of metalloproteinase-2, metalloproteinase-9, and tissue inhibitor of metalloproteinase-1 in transitional cell carcinoma of upper urinary tract: correlation with tumor stage and survival. Urology 2004;63:602–8.
17. Dinney CP, Babkowski RC, Antelo M, Perrotte P, Liebert M, Zhang HZ, et al. Relationship among cystectomy, microvessel density and prognosis in stage T1 transitional cell carcinoma of the bladder. J Urol 1998;160:1285–90.
18. Theodoropoulos VE, Lazaris ACh, Sofras F, Gerzelis I, Tsoukala V, Ghikonti I, et al. Hypoxia-inducible factor 1 alpha expression correlates with angiogenesis and unfavorable prognosis in bladder cancer. Eur Urol 2004;46:200–8.
19. Offersen BV, Knap MM, Marcussen N, Horsman MR, Hamilton-Dutoit S, Overgaard J. Intense inflammation in bladder carcinoma is associated with angiogenesis and indicates good prognosis. Br J Cancer 2002;87:1422–30.
20. Watanabe K, Hasegawa Y, Yamashita H, Shimizu K, Ding Y, Abe M, et al. Vasohibin as an endothelium-derived negative feedback regulator of angiogenesis. J Clin Invest 2004;114:898–907.
21. Kimura H, Miyashita H, Suzuki Y, Kobayashi M, Watanabe K, Sonoda H, et al. Distinctive localization and opposed roles of vasohibin-1 and vasohibin-2 in the regulation of angiogenesis. Blood 2009;113:4810–8.
22. Hosaka T, Kimura H, Heishi T, Suzuki Y, Miyashita H, Ohta H, et al. Vasohibin-1 expression in endothelium of tumor blood vessels regulates angiogenesis. Am J Pathol 2009;175:430–9.
23. Yoshinaga K, Ito K, Moriya T, Nagase S, Takano T, Niikura H, et al. Roles of intrinsic angiogenesis inhibitor, vasohibin, in cervical carcinomas. Cancer Sci 2011;102:446–51.
24. Mikami S, Oya M, Mizuno R, Murai M, Mukai M, Okada Y. Expression of Ets-1 in human clear cell renal cell carcinomas: implications for angiogenesis. Cancer Sci 2006;97:875–82.
25. Tamaki K, Moriya T, Sato Y, Ishida T, Maruo Y, Yoshinaga K, et al. Vasohibin-1 in human breast carcinoma: a potential negative feedback regulator of angiogenesis. Cancer Sci 2009;100:88–94.
26. Tamaki K, Sasano H, Maruo Y, Takahashi Y, Miyashita M, Moriya T, et al. Vasohibin-1 as a potential predictor of aggressive behavior of ductal carcinoma *in situ* of the breast. Cancer Sci 2010;101:1051–8.
27. Chung AS, Lee J, Ferrara N. Targeting the tumour vasculature: insights from physiological angiogenesis. Nat Rev Cancer 2010;10:505–14.
28. Sato Y, Sonoda H. The vasohibin family: a negative regulatory system of angiogenesis genetically programmed in endothelial cells. Arterioscler Thromb Vasc Biol 2007;27:37–41.
29. Shibuya T, Watanabe K, Yamashita H, Shimizu K, Miyashita H, Abe M, et al. Isolation and characterization of vasohibin-2 as a homologue of VEGF-inducible endothelium-derived angiogenesis inhibitor vasohibin. Arterioscler Thromb Vasc Biol 2006;26:1051–7.
30. Yoshinaga K, Ito K, Moriya T, Nagase S, Takano T, Niikura H, et al. Expression of vasohibin as a novel endothelium-derived angiogenesis inhibitor in endometrial cancer. Cancer Sci 2008;99:914–9.

Published OnlineFirst July 23, 2012; DOI: 10.1158/1541-7786.MCR-12-0098-T

Angiogenesis, Metastasis, and the Cellular Microenvironment

Molecular Cancer Research

Vasohibin-2 Expressed in Human Serous Ovarian Adenocarcinoma Accelerates Tumor Growth by Promoting Angiogenesis

Yoshifumi Takahashi[1,2], Takahiro Koyanagi[1,2], Yasuhiro Suzuki[1], Yasushi Saga[2], Naoki Kanomata[3], Takuya Moriya[3], Mitsuaki Suzuki[2], and Yasufumi Sato[1]

Abstract

Vasohibin-1 (VASH1) is a VEGF-inducible endothelium-derived angiogenesis inhibitor and VASH2 is its homolog. Our previous analysis revealed that VASH1 is expressed in endothelial cells to terminate angiogenesis, whereas VASH2 is expressed in infiltrating mononuclear cells mobilized from bone marrow to promote angiogenesis in a mouse model of hypoxia-induced subcutaneous angiogenesis. To test the possible involvement of VASH2 in the tumor, we examined human ovarian cancer cells for the presence of VASH2. Immunohistochemical analysis revealed that VASH2 protein was preferentially detected in cancer cells of serous ovarian adenocarcinoma. We then used SKOV-3 and DISS, two representative human serous adenocarcinoma cell lines, and examined the role of *VASH2* in the tumor. The knockdown of VASH2 showed little effect on the proliferation of cancer cells *in vitro* but notably inhibited tumor growth, peritoneal dissemination, and tumor angiogenesis in a murine xenograft model. Next, we stably transfected the human *VASH2* gene into two types of murine tumor cells, EL-4 and MLTC-1, in which endogenous VASH2 was absent. When either EL-4 or MLTC-1 cells were inoculated into *VASH2* (−/−) mice, the VASH2 transfectants formed bigger tumors when compared with the controls, and the tumor microvessel density was significantly increased. VASH2 stimulated the migration of endothelial cells, and its increased expression in cancer cells is related to the decrease of mir-200b. These results indicate that VASH2 expressed in serous ovarian carcinoma cells promoted tumor growth and peritoneal dissemination by promoting angiogenesis. *Mol Cancer Res; 10(9); 1135–46. ©2012 AACR.*

Introduction

Ovarian cancer is the second most common malignant tumor in gynecology and is the leading cause of cancer-related death for women worldwide (1). Cytotoxic therapy with platinum and taxanes is initially effective in many cases of ovarian cancer, but there is a considerable risk of recurrence and resistance to such cytotoxic therapy (2). Thus, it is critical to develop alternative options that target pathways responsible for the progression of ovarian cancer. Angiogenesis is recognized as one of the principal hallmarks of various cancers (3). Indeed, tumor angiogenesis is thought to be a key process that enables ovarian cancer growth as well as dissemination in the peritoneal space, and thus one of the promising options for treating ovarian cancer is considered to be antiangiogenic therapy (4).

Ovarian cancer cells express various angiogenesis stimulators (1). Among them, VEGF plays the most important role, as it stimulates the migration and proliferation of, and tube formation by, endothelial cells. VEGF is the prototype of the VEGF family, and its proangiogenic signals are mainly transmitted via its type 2 receptor (VEGFR2) on endothelial cells (5). High levels of VEGF have been found in ovarian cancers, which is associated with poor survival of patients in both early and advanced stages of the disease (6, 7). In animal models of ovarian cancer, inhibition of VEGF reduces tumor growth and inhibits ascites accumulation (8). It is suggested that VEGF may also promote tumor growth by direct action on VEGF receptors expressed on ovarian cancer cells (9). Angiopoietins and their receptor, TIE2, are another ligand receptor system that regulates angiogenesis. Angiopoietin-1 (Ang-1) is an agonistic ligand of TIE2, and it facilitates pericyte covering of vessels for vascular stabilization, whereas Ang-2 is an antagonistic of ligand of TIE2 and induces detachment of pericytes from vessels for vascular destabilization (10). An increase in the Ang-2 level in cancers may be related to the immature phenotype of tumor vessels.

Authors' Affiliations: [1]Department of Vascular Biology, Institute of Development, Aging, and Cancer, Tohoku University, Sendai; [2]Department of Obstetrics and Gynecology, School of Medicine, Jichi Medical University, Tochigi; and [3]Department of Pathology 2, Kawasaki Medical University, Kurashiki, Japan

Note: Supplementary data for this article are available at Molecular Cancer Research Online (http://mcr.aacrjournals.org/).

Corresponding Author: Yasufumi Sato, Department of Vascular Biology, Institute of Development, Aging, and Cancer, Tohoku University, 4-1 Seiryo-machi, Aoba-ku, Sendai 980-8575, Japan. Phone: 81-022-717-8528; Fax: 81-022-717-8533; E-mail: y-sato@idac.tohoku.ac.jp

doi: 10.1158/1541-7786.MCR-12-0098-T

Published OnlineFirst July 23, 2012; DOI: 10.1158/1541-7786.MCR-12-0098-T

Regarding these 2 angiopoietins, the serum Ang-2 level is significantly high in patients with ovarian cancer and is proposed to be a biomarker of malignant potential and poor prognosis in ovarian cancer (11).

The local balance between angiogenesis stimulators and inhibitors determines the occurrence and progress of angiogenesis. We recently isolated vasohibin-1 (VASH1) as a negative feedback regulator of angiogenesis that is induced in endothelial cells by angiogenesis stimulators such as VEGF and fibroblast growth factor 2 (FGF-2; refs. 12, 13). By conducting a database search, we found one gene homologous to VASH1 and named it VASH2 (14). The amino acid sequence of the human VASH2 protein is 52.5% homologous to that of human VASH1, and both VASH1 and VASH2 are highly conserved among species. VASH1 and VASH2 lack the classical signal sequence; but they bind to the small intracellular vasohibin-binding protein (SVBP), and this binding with SVBP facilitates their secretion (15). Because of the similarity between VASH1 and VASH2, we examined their expression and function by the use of hypoxia-induced subcutaneous angiogenesis in mice. Our analysis revealed that VASH1 is mainly expressed in endothelial cells in the termination zone to halt angiogenesis, whereas VASH2 is mainly expressed in mononuclear cells mobilized from the bone marrow in the sprouting front to stimulate angiogenesis (16). Thus, these 2 VASH family members regulate angiogenesis perhaps in a seemingly contradictory manner.

Previously, we investigated the expression of VASH1 under conditions accompanied by conducive to pathologic angiogenesis and showed its presence in endothelial cells of various cancers (17–21), atherosclerotic lesions (22), age-dependent macular degeneration (23), and diabetic retinopathy (24). However, the expression of VASH2 is ill-defined. Here, we conducted immunohistochemical analysis of VASH2 in ovarian cancers and showed for the first time the expression of VASH2 in them. This expression seems to be restricted to serous adenocarcinoma of the ovary. Our subsequent analysis indicated that VASH2 in ovarian cancer cells promoted tumor growth and peritoneal dissemination via the stimulation of angiogenesis.

Materials and Methods

Immunohistochemical analysis of VASH2 in ovarian cancer

This study was approved by the ethics committee of Jichi Medical University Hospital (Tochigi, Japan). Twenty-one patients with epithelial ovarian carcinoma who underwent surgery at Jichi Medical University Hospital between 2007 and 2009 were included in this study. Histologic types were assigned according to the criteria of the World Health Organization (WHO) classification.

Paraffin-embedded blocks of cancer tissue were prepared, and thin sections were cut and placed on glass slides. After deparafinization and hydration, endogenous peroxidase activity was quenched by a 5-minutes incubation in 3% hydrogen peroxide. The sections were then incubated for 1 hour at room temperature with anti-VASH2 mAb (14) at the concentration of 2 μg/mL. The samples were washed with Tris-buffered saline, and the color was developed using the EnVision$^+$System (Dako), according to the manufacturer's instructions. Sections were counterstained with hematoxylin and mounted. A sample from which the primary antibody was omitted served as the negative control.

Cells and cell culture

The human ovarian serous adenocarcinoma cell line SKOV-3 (25) was purchased from American Type Culture Collection (ATCC), and the DISS one was described previously (26). The murine lymphoma cell line EL-4 and murine Lewis lung carcinoma (LLC) were provided from the Cell Resource Center for Biomedical Research, Institute of Development, Aging, and Cancer, Tohoku University (Sendai, Japan). The murine malignant melanoma cell line B16F1 and murine Leydig tumor cell line MLTC-1 were purchased from ATCC. The murine fibrosarcoma cell line 505-05-01 and the murine ovarian carcinoma cell line OV2944-HM-1 were purchased from RIKEN Cell Bank (Tsukuba, Japan). These cell lines were maintained in Dulbecco's Modified Eagle Medium (DMEM; Wako) supplemented with 10% heat-inactivated fetal calf serum (FCS; JRH Biosciences and 100 μg/mL kanamycin (Meiji Seika Kaisha Ltd.). Human umbilical vein endothelial cells (HUVEC) and human microvascular endothelial cells (HMVEC) were obtained from Kurabo Industries, Ltd. and were cultured on type I collagen-coated dishes (IWAKI) in endothelial basal medium EBM-2 (Lonza) supplemented with EGM-2-MV-SingleQuots (Lonza) containing VEGF, FGF-2, insulin-like growth factor-I, EGF, and 5% FBS. MS1, an immortalized cell line with a SV40 large T antigen from mouse pancreatic endothelial cells, was purchased from ATCC and was cultured in αMEM (Wako) supplemented with 10% FCS. Human ovarian epithelial cells (HOEC) were purchased from ScienCell Research Laboratories, and were cultured on poly-L-lysine–coated dishes (IWAKI) in ovarian epithelial cell medium (ScienCell) supplemented with ovarian epithelial cell growth supplement (ScienCell).

All the cells were cultured at 37°C in a humidified atmosphere with 5% CO_2.

Knockdown of VASH2 by short hairpin RNA

The short hairpin RNA (shRNA) sequence that suppresses VASH2 expression is 5′-CACCAGGTGATCTAGAATT-GCATACGTGTGCTGTCCGTATGTAATTCTGGAT-CGCCTTTTTT. This sequence was inserted into the piGENE hU6 Vector (iGENE) to make the VASH2 shRNA expression vector. Cells were transfected with this vector or control vector by using Effectene transfection reagent. After the transfection, the cells were selected in puromycin (Calbiochem)-containing medium; and the bulk cells were obtained. Next, the bulk cells were seeded at a density of 0.3 cells per well in 96-well plates with 100 μL medium per well, and visible clones were picked and expanded in 24-well plates. These clones were finally transferred to regular cell culture flasks, and the VASH2 knockdown clones were thus established.

Published OnlineFirst July 23, 2012; DOI: 10.1158/1541-7786.MCR-12-0098-T

Establishment of VASH2-expressing murine tumor cell clones

Human *VASH2* cDNA was cloned into the pCALL2-pcDNA3.1/Hygro vector at multiple cloning sites (*Xho*I and *Not*I). To improve the activity of transcription, we replaced the cytomegalovirus (CMV) promoter of the pcDNA3.1/Hygro plasmid (Invitrogen) with the chicken *β-actin* promoter derived from pCALL2 (27). Cells were transfected with the *VASH2* expression vector or control vector by using Effectene transfection reagent (QIAGEN) according to the manufacturer's protocol. After the transfection, the cells were selected in hygromycin (Invitrogen)-containing medium, and the clones having high VASH2 expression were established according to the procedure similar to that for the selection of the VASH2 knockdown clones.

Reverse transcriptase PCR

Total RNA was extracted from cell cultures by using an RNeasy mini kit (QIAGEN) according to the manufacturer's instructions. Total tissue RNA was extracted from tumors with ISOGEN (Nippon Gene) according to the manufacturer's instructions. First-strand cDNA was generated by using ReverTra Ace (TOYOBO). The reverse transcriptase PCR (RT-PCR) procedure was carried out in a DNA thermal cycler (Takara). PCR conditions consisted of an initial denaturation step at 95°C for 5 minutes followed by 25 to 35 cycles consisting of 15 seconds at 95°C, 15 seconds at the appropriate annealing temperature, and 30 seconds at 72°C. PCR products were separated on a 1.5% agarose gel and visualized under ultraviolet by ethidium bromide staining. The primer pairs used were as follow: mouse *β-actin* forward, 5′-TCGTGCGTGACATCAAAGAG, and reverse, 5′-TGGACAGTGAGGCCAGGATG (annealing temperature: 58°C); human *β-actin* forward, 5′-ACAATGAGCTGCGTGTGGCT, and reverse, 5′-TCGTGCGTGACATTAAGGAGA (annealing temperature: 58°C); mouse *VASH2* forward, 5′-TGGAGACAGCGAAGGAGATG, and reverse, 5′-GAAGCAACTTGTCCTCAACG (annealing temperature: 56°C); human *VASH2* forward, 5′-AGCTGATGGACAAGCCATTG, and reverse, 5′-CTCTGAATGAAGTGGGCTATC (annealing temperature: 56°C).

Transient transfection with anti-miR or pre-miR

SKOV-3 cells were grown to 60% to 70% confluence and then transfected with 50 nmol/L anti-miR-200b (Ambion), pre-miR-200b (Ambion), or their negative control oligonucleotides (Ambion) by using Lipofectamine RNAiMAX (Invitrogen) according to the manufacturer's instructions. The medium was changed after 12 hours of transfection, and the cells cultured for an additional 48 hours.

Quantitative real-time RT-PCR of VASH2 and miR-200b

Total RNA was extracted from HOECs, ovarian cancer cells, and ovarian cancer tissues using RNeasy Mini Kit. First-strand cDNA was generated using ReverTra Ace for RT-PCR. Quantitative real-time RT-PCR was carried out using the CFX96 real-time PCR detection system (Bio-Rad Laboratories) according to the manufacturer's instructions. PCR conditions consisted of an initial denaturation step at 95°C for 3 minutes, followed by 40 cycles of 10 seconds at 95°C, 10 seconds at 56°C, and 30 seconds at 72°C. Each mRNA level was measured as a fluorescent signal corrected according to the signal for *β-actin*. The primer pairs used were as follows: human VASH2 forward, 5′-TGCACACAGTCAAGAAGGTC-3′, and reverse, 5′-TTCTCACTTGGGTCGGAGAG-3′; human *β-actin* forward, 5′-ACAATGAGCTGCGTGTGGCT-3′, and reverse, 5′-TCTCCTTAATGTCACGCACGA-3′. miR-200b levels were analyzed by the TaqMan real-time PCR method. Ten nanograms of total RNA was reverse transcribed by using a TaqMan MicroRNA Reverse Transcription kit (Applied Biosystems) according to the manufacturer's instructions. The specific primer for miR200b was designed and produced by Applied Biosystems. Real-time PCR was carried out with the CFX96 real-time PCR detection system. PCR conditions consisted of an initial denaturation step at 95°C for 10 minutes, followed by 40 cycles of 15 seconds at 95°C and 60 seconds at 60°C. Relative expression levels were calculated by using the comparative C_t method.

Proliferation of tumor cells

Proliferation of tumor cells was measured by conducting the Tetra Color ONE cell proliferation assay (28). Briefly, the cells were seeded at a density of 3×10^3 cells per well in a 96-well plate and incubated at 37°C. After 48 hours, 5 μL of Tetra Color ONE (Seikagaku Co.) was added to each well; and mixture was then incubated for an additional 2 hours. Absorbance at 450 nm was monitored.

Proliferation of endothelial cells

VASH2-expressing EL-4 clone or EL-4 cells transfected with empty vector were cultured at 1×10^6 cells/mL for 24 hours and centrifuged at 1,000 rpm for 5 minutes to obtain the conditioned medium (CM). Next, the cellular components were removed from the CM by using a MILLEX-GP PES 0.22-μm filter (Millipore) and concentrated 10-fold with a VIVASPIN15; MWCO 10,000 (Sartorius Stedim Biotech). MS1 cells were plated in a 96-well plate at 2×10^3 cells per well and cultured in medium to which the CM had been added, and the proliferation was measured by using the Tetra Color ONE.

Migration of endothelial cells

The migratory activity of endothelial cells was measured by use of the modified Boyden chamber method. MS1 cells were preincubated in 1% FCS in α-MEM for 24 hours and then plated at 5×10^5 cells/mL on the upper chamber (insert) of a Boyden chamber (8.0-μm pore size, Corning). The low chamber was filled with CM corrected from *VASH2* gene or mock transfectants as described above. MS1 cells were allowed to migrate for 6 hours, the cells that had migrated across the filter were

Published OnlineFirst July 23, 2012; DOI: 10.1158/1541-7786.MCR-12-0098-T

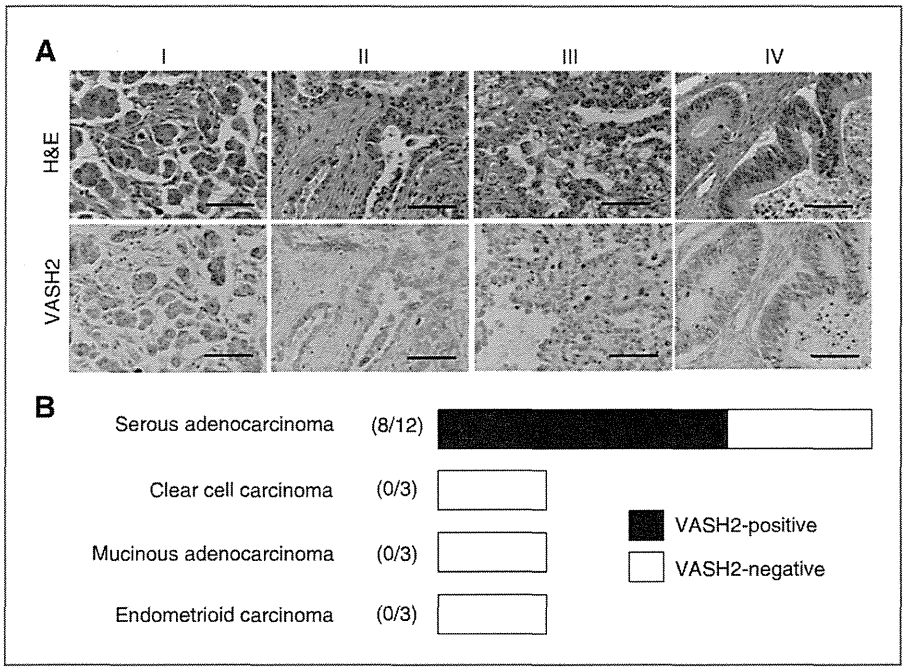

Figure 1. Expression of VASH2 in human serous ovarian adenocarcinoma cells. A, histologic analysis of human ovarian adenocarcinoma was conducted. I and II, serous ovarian adenocarcinoma; III, clear cell carcinoma; and IV, mucinous adenocarcinoma. Top, hematoxylin and eosin (H&E) staining. Bottom, VASH2 immunostaining. Bar, 100 μm. B, eight of 12 cases were positive for VASH2 in serous ovarian adenocarcinoma. Three cases of clear cell carcinoma, 3 cases of mucinous adenocarcinoma, and 3 cases of endometrioid carcinoma were all negative for VASH2.

stained with Difu Quick (Sysmex), and the number of cells that had migrated was counted in 5 fields per insert in a blind manner.

Mouse xenograft models

Female 6- to 8-week-old BALB/c nude mice were obtained from Clea Laboratories. *VASH2*$^{-/-}$ mice on a C57BL/6 background were previously described (16). All of the animal experiments were approved by Tohoku University Center for Gene Research and carried out under the guidelines for animal experimentation of Tohoku University.

Subcutaneous tumor growth

Tumor cells were subcutaneously transplanted into the back of mice at 2×10^6 cells per mouse. Two dimensions of the tumors were measured every 3 days by using a caliper. The tumor volume was calculated by the formula: volume = (short diameter)^2 × (long diameter) × 1/2.

Peritoneal dissemination, ascites accumulation, and survival rate

Tumor cells were intraperitoneally injected into BALB/c nude mice at 2×10^6 cells per mouse. Two or 3 weeks after the injection, the mice were sacrificed. Thereafter, the ascites fluid was collected, and its volume was measured. Peritoneal dissemination was evaluated by counting the number of tumor nodes on the surface of the small intestines and mesentery. The survival of the mice was monitored twice daily. The survival rate was calculated by the Kaplan–Meier method.

Orthotopic inoculation of ovarian cancer cells

Orthotopic tumor cell inoculation was conducted according to the method described by Cordero and colleagues. (29). Briefly, a small incision was made at the dorsomedial position and directly above the ovarian fat pad. The ovarian fat pad was gently pulled out and cancer cells (1×10^5) were inoculated between the brusa and the ovary. Thirty-two days after the inoculation, mice were sacrificed and tumors in the ovary were examined.

Immunohistochemical analysis

For immunohistochemical analysis, tumors were frozen in optimum cutting temperature (OCT) compound (Sakura), cut into 7-μm sections, fixed in methanol for 20 minutes at −20°C, and blocked with 1% bovine serum albumin in PBS for 30 minutes at room temperature. Primary antibody reactions were conducted overnight at 4°C with rat monoclonal antibody against mouse CD31 (Research Diagnostics) at a dilution of 1:500, mouse monoclonal antibody against mouse αSMA (Sigma-Aldrich) at a dilution of 1:200. Secondary antibody reactions were conducted for 1 hour at room temperature with Alexa Fluor 488–conjugated donkey anti-rat IgG, Alexa Fluor 568–conjugated goat anti-rat IgG, Alexa Fluor 555–conjugated goat anti-mouse IgG (Molecular Probes) at a dilution of 1:500. After having been washed

Published OnlineFirst July 23, 2012; DOI: 10.1158/1541-7786.MCR-12-0098-T

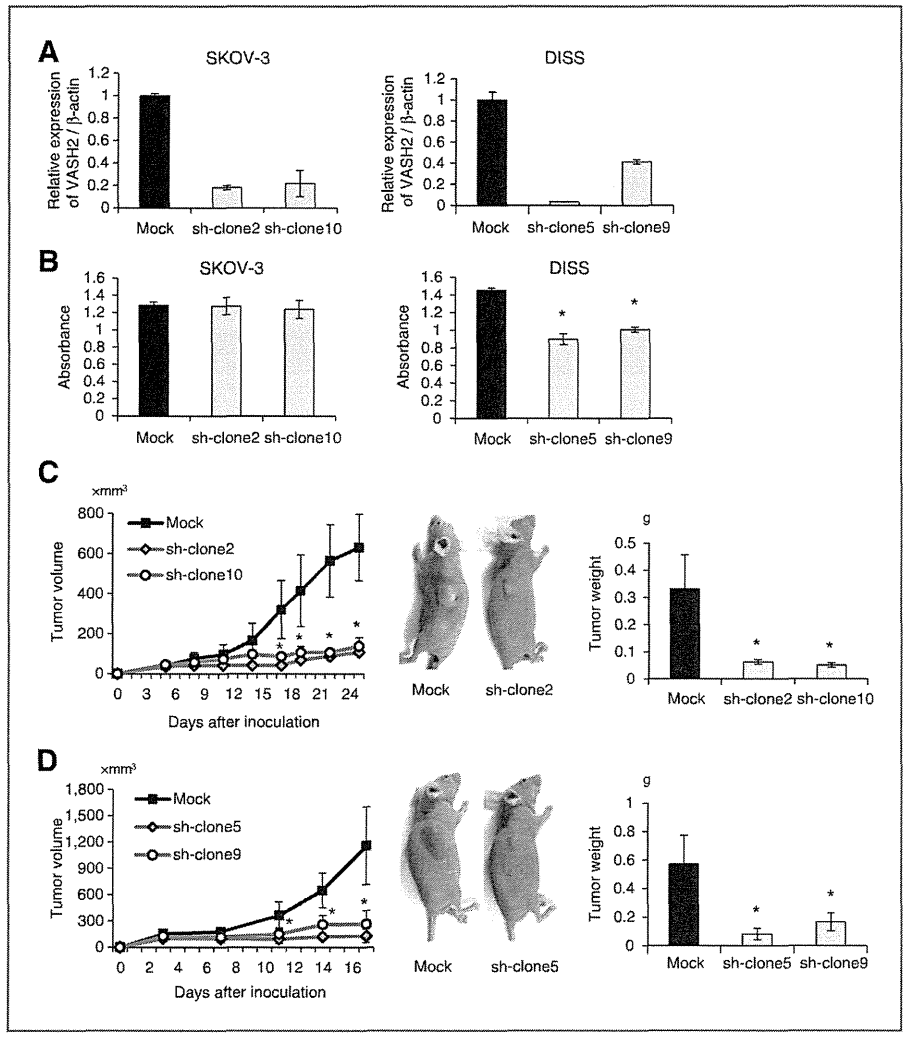

Figure 2. Knockdown of VASH2 inhibited subcutaneous tumor growth. A, two VASH2 knocked-down (sh-VASH2) clones (sh-clone2 and sh-clone10) from SKOV-3, 2 from DISS (sh-clone5 and sh-clone9), and their control mock transfectants were established. Their expression of VASH2 was determined by quantitative RT-PCR. Means and SDs are shown ($N = 3$). B, proliferation of sh-VASH2 clones and of their control mock transfectant was compared under the same cell culture conditions. Means and SDs are shown ($N = 3$). *, $P < 0.01$ versus mock. C, two sh-VASH2 clones (sh-clone2 and sh-clone10) or their control mock established from SKOV-3 cells were inoculated subcutaneously into nude mice, and the serial tumor growth was compared in terms of tumor volume and weight. Means and SDs are shown ($N = 5$). *, $P < 0.01$ versus mock. Twenty-five days after the inoculation, photographs were taken, and the tumor weight was measured. Mean and SDs are shown ($N = 5$). *, $P < 0.01$ versus mock. D, two sh-VASH2 clones (sh-clone5 and sh-clone9) or their control mock established from DISS were inoculated subcutaneously into nude mice and the serial tumor growth was compared as in C. Means and SDs are shown ($N = 4$). *, $P < 0.01$. Seventeen days after the inoculation, photographs were taken, and tumor weight was measured. Mean and SDs are shown ($N = 4$). *, $P < 0.01$ versus mock.

3 times with PBS, the sections were covered with fluorescent mounting medium. All samples were analyzed with a BZ-9000 fluorescence microscope (KEYENCE) with a ×10, ×20, ×40, ×100 objective lens at room temperature. The vascular luminal area was calculated from 5 different fields. Quantitative analyses of vessels and cells were done by using BZ-H1C software (KEYENCE) and ImageJ software (http://rsbweb.nih.gov/ij/).

Quantification of proliferating cancer cells *in vivo*

Deparaffinized and rehydrated tumor tissue sections were incubated overnight at 4°C with anti–proliferating cell nuclear antigen (PCNA) antibody (Santa Cruz Biotechnology) at a dilution of 1:200. The samples were incubated in biotin-conjugated antibody solution and streptavidin followed by staining with 3,3′-diaminobenzidine (DAB). The sections were then counterstained with Mayer hematoxylin, and the percentage of PCNA-positive cells was quantified by using HistoQuest software (NOVEL SCIENCE).

Quantification of apoptotic cancer cells *in vivo*

To evaluate apoptotic cancer cells, we conducted terminal deoxynucleotidyl transferase–mediated dUTP nick end labeling (TUNEL) staining. Deparaffinized and rehydrated tumor tissue sections were immersed in protease solution and were incubated with terminal deoxynucleotidyl transferase to label 3′ terminals of DNA. Then, they were incubated in peroxidase-conjugated antibody solution and were stained with DAB. The sections were counterstained with methyl green, and the percentage of TUNEL-positive cells was quantified by using HistoQuest software (NOVEL SCIENCE).

Statistical analysis

The statistical significance of differences was evaluated by unpaired ANOVAs, and probability values were calculated with the Student t test. Survival rates were analyzed by the generalized Wilcoxon and log-rank tests. $P < 0.05$ was considered statistically significant.

Published OnlineFirst July 23, 2012; DOI: 10.1158/1541-7786.MCR-12-0098-T

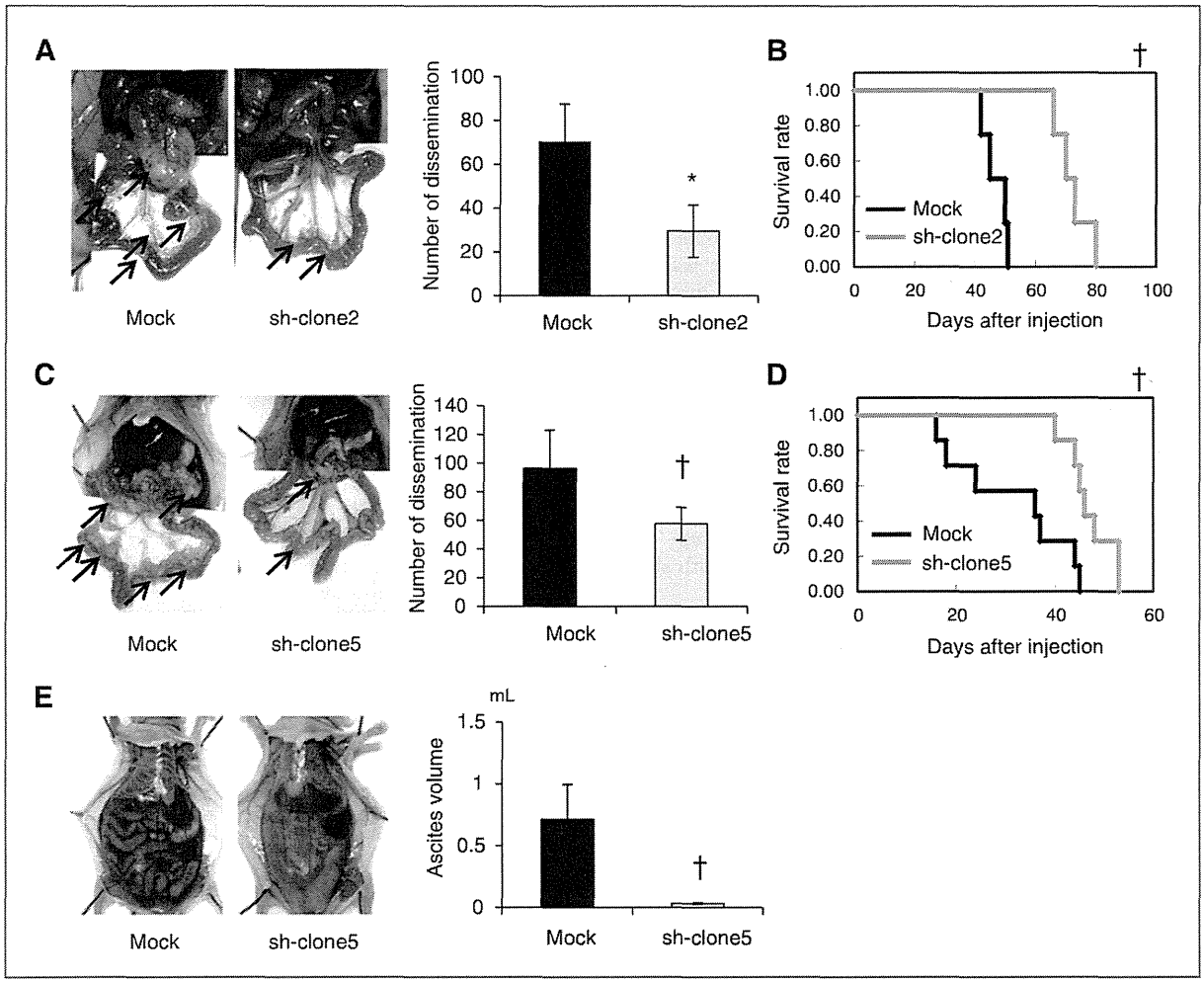

Figure 3. Knockdown of VASH2 inhibited peritoneal dissemination of tumor cells and improved survival rate *in vivo*. A, sh-clone2 or mock transfectant cells established from SKOV-3 were injected into nude mice by the intraperitoneal route. Three weeks after the injection, the mice were sacrificed; and then peritoneal dissemination of the tumor cells was determined. Mean and SDs are shown ($N = 4$). *, $P < 0.01$ versus mock. B, after the injection of sh-clone2 or mock transfectant established from SKOV-3, the survival of the mice was monitored twice daily ($N = 4$). †, $P < 0.05$ versus mock. C, sh-clone5 or mock transfectant cells established from DISS were injected into nude mice intraperitoneally. Two weeks after the injection, the mice were sacrificed; and peritoneal tumors were counted. Mean and SDs are shown ($N = 3$). †, $P < 0.05$ versus mock. D, after the injection of sh-clone5 or mock transfectant cells established from DISS, the survival of the mice was monitored twice daily ($N = 7$). †, $P < 0.05$ versus mock. E, sh-clone5 or mock transfectant cells established from DISS were injected into nude mice intraperitoneally. Two weeks after the injection, the mice were sacrificed, after which the volume of ascites was measured. Mean and SDs are shown ($N = 3$). †, $P < 0.05$ versus mock.

Results

VASH2 is expressed in human serous ovarian carcinoma cells

To test the possible involvement of VASH2 in the tumor, we analyzed human ovarian cancers for its presence. Immunohistochemical analysis of the pathologic sections revealed that VASH2 protein was preferentially detected in serous ovarian adenocarcinoma cells (Fig. 1A). Indeed, cancer cells in 8 of 12 cases of serous ovarian adenocarcinoma (67%) were positive for VASH2, whereas cancer cells in all of the cases of non–serous ovarian adenocarcinoma; that is, 3 cases of clear cell carcinoma, 3 cases of mucinous adenocarcinoma, and 3 cases of endometrioid carcinoma, were negative for it (Fig. 1B).

Knockdown of VASH2 in cancer cells decreases tumor growth via the inhibition of tumor angiogenesis

To verify the function of VASH2 in ovarian cancers, we conducted a loss-of-function experiment by knocking down the expression of VASH2. We used SKOV-3 and DISS for the following experiments, as they are representative ovarian cancer cells that are highly tumorigenic in animals. At least, 7 variant transcripts of human VASH2 are registered in the database (Supplementary Fig. S1). We designed shRNAs to knock down most of the splicing variants and established 2 VASH2 knocked-down (sh-VASH2) clonal cell lines from each of SKOV-3 and DISS (Fig. 2A). The knockdown of VASH2 did not alter the *in vitro* proliferation of SKOV-3 but slightly decreased that

Published OnlineFirst July 23, 2012; DOI: 10.1158/1541-7786.MCR-12-0098-T

of DISS (Fig. 2B). We then inoculated either of these VASH2-knocked down cancer cells subcutaneously into nude mice and observed a significant reduction in tumor growth in terms of both tumor volume and weight (Fig. 2C and D).

Peritoneal dissemination often occurs in serous adenocarcinoma of the ovary and is a sign of poor prognosis. We injected cancer cells into the peritoneal cavity as a model of peritoneal dissemination and observed that there was a significant decrease in the number of disseminated tumors in mice injected with SKOV-3 or DISS cells that had been transfected with sh-VASH2 (Fig. 3A and C). In addition, DISS cells caused the accumulation of a bloody ascites, but it was almost completely abrogated by sh-VASH2 (Fig. 3E). As the result, the survival period was prolonged in mice that had been injected with either SKOV-3 or DISS sh-VASH2 cells (Fig. 3B and D).

We further examined an orthotopic mouse model. Again we observed a significant reduction in tumor growth of SKOV-3 or DISS cells that had been transfected with sh-VASH2 (Fig. 4).

We previously reported that VASH1 inhibits angiogenesis whereas VASH2 promotes it (16). We therefore examined the vasculature in the tumors and found a significant decrease in angiogenesis in tumors derived from either SKOV-3 or DISS sh-VASH2 cells (Fig. 5A and C). The decrease of tumor angiogenesis resulted in the significant increase of cancer cell apoptosis but no changes in cancer cell proliferation *in vivo* (Supplementary Fig. S2). We further investigated the vascular composition of endothelial cells and mural cells. The association of mural cells with endothelial cells was not significantly altered in either type of tumor (Fig. 5B and D). We did not observe any differences in the extent of mural cell coverage in tumor vessels (Fig. 5B).

Expression of VASH2 in cancers increases tumor growth via the promotion of tumor angiogenesis

To further confirm proangiogenic function of VASH2 in tumors, we carried out a gain-of-function experiment by introducing the VASH2 gene in cancer cells. VASH2 can be expressed in bone marrow–derived $CD11b^{+}$ mononuclear cells (16). To avoid the possible involvement of recipient VASH2, we planned to use *VASH2* (−/−) mice. As our *VASH2* (−/−) mice were on a C57BL6 background, we examined various tumorigenic C57BL6 murine tumor cells and found that EL-4 and MLTC-1 did not express endogenous VASH2 (Supplementary Fig. S2). We introduced the human *VASH2* gene into EL-4 and established stable clones (Fig. 6A). The introduction of the *VASH2* gene slightly but significantly inhibited the *in vitro* proliferation of these tumor cells (Fig. 6B). We then inoculated these cells subcutaneously into *VASH2* (−/−) mice. Parental EL-4 cells are tumorigenic, indicating that they have sufficient angiogenic activity despite of the lack of VASH2 expression. Even though the *VASH2* gene slightly decreased the proliferation of tumor cells, we observed a significant intensification of tumor growth in VASH2 transfectants (Fig. 6C). Then, we examined the vasculature in the tumors. As expected, tumors of mock transfectants contained a certain quantity of tumor vessels. Nevertheless, we observed that there was a significant increase in tumor angiogenesis, as evidenced by the increased vascular luminal area, in the VASH2 transfectants (Fig. 6D). We further observed that the association of mural cell with endothelial cells was not significantly altered in the EL-4 transfectants (Fig. 6E).

VASH2 affects both endothelial cells and cancer cells to promote angiogenesis

VASH1 exhibits its antiangiogenic activity by inhibiting migration and proliferation of endothelial cells (12). As a

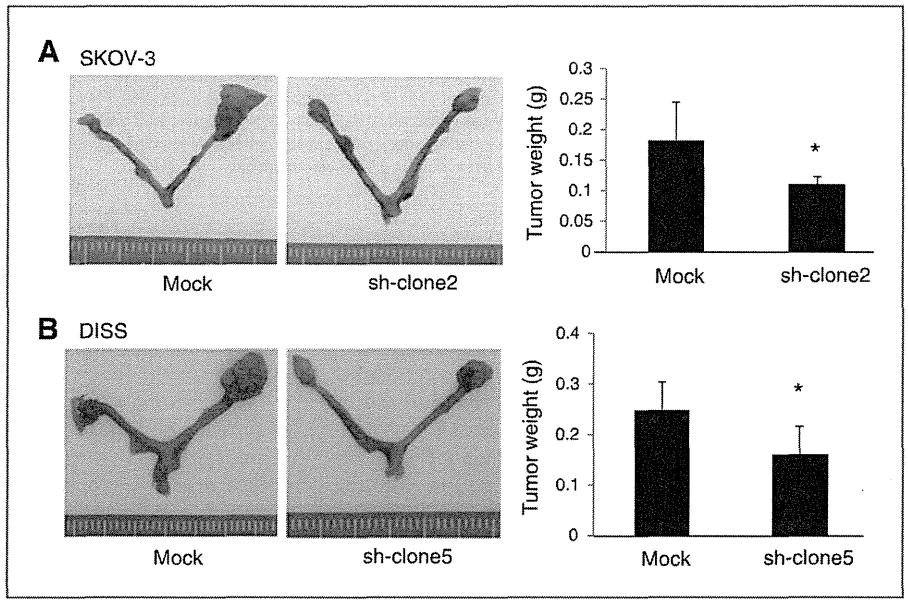

Figure 4. Knockdown of VASH2 inhibited orthotopic tumor growth. A, sh-clone2 or mock transfectant cells (1×10^5 cells) established from SKOV-3 were orthotopically inoculated into nude mice. Thirty-two days after the inoculation, the mice were sacrificed; and then the tumor size was determined. Mean and SDs are shown ($N = 5$). *, $P < 0.05$ versus mock. B, sh-clone5 or mock transfectant cells (1×10^5 cells) established from DISS were orthotopically inoculated into nude mice. Thirty-two days after the inoculation, the mice were sacrificed; and then the tumor size was determined. Mean and SDs are shown ($N = 5$). *, $P < 0.05$ versus mock.

Published OnlineFirst July 23, 2012; DOI: 10.1158/1541-7786.MCR-12-0098-T

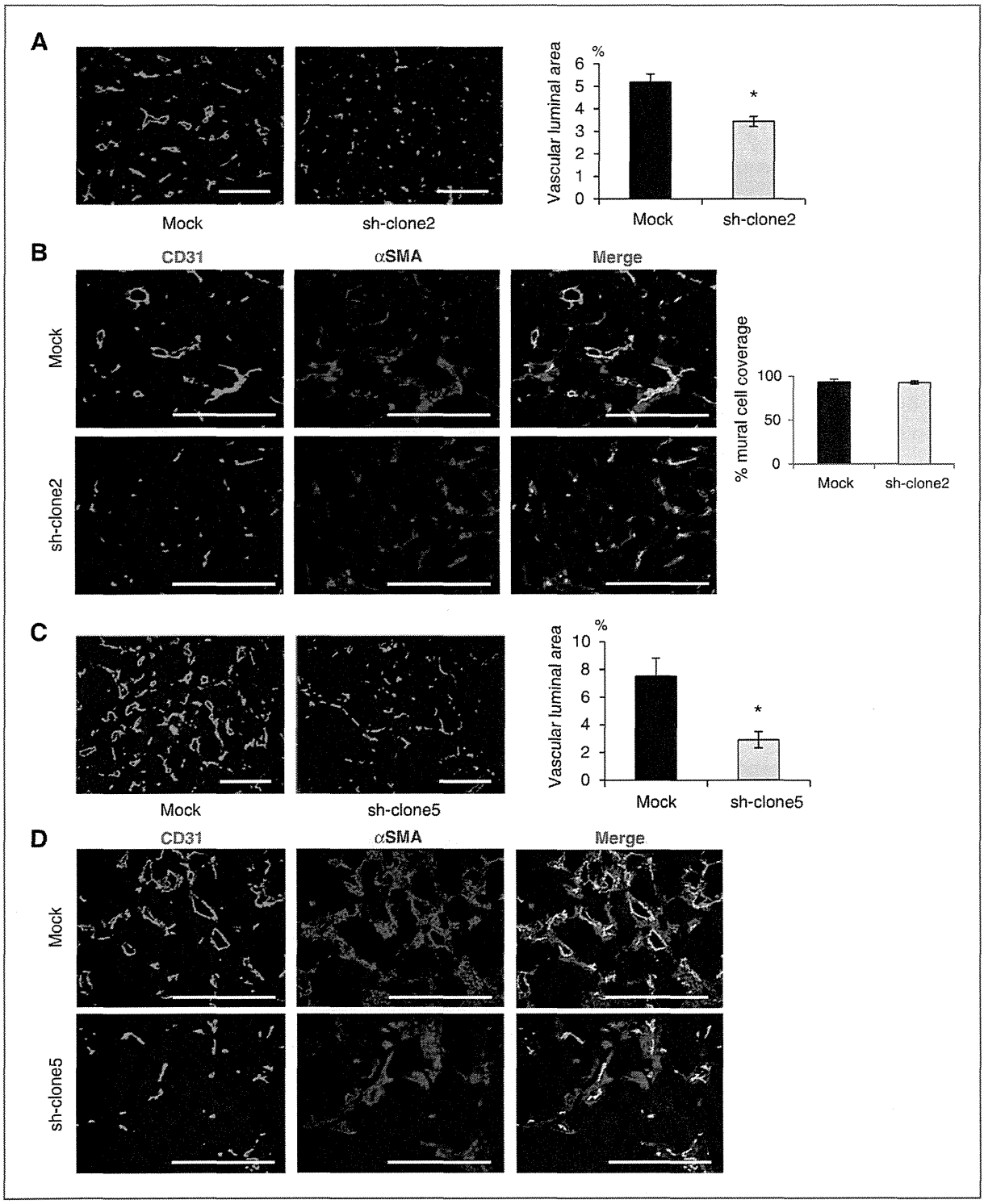

Figure 5. Knockdown of VASH2 inhibited tumor angiogenesis. A, sections of tumors formed by sh-clone2 or mock transfectants established from SKOV-3 were immunostained with anti-CD31. Bar, 300 μm. The vascular luminal area was calculated on the basis of area in 5 different fields. Mean and SDs are shown ($N = 3$). *, $P < 0.01$ versus mock. B, sections of tumors generated from sh-clone2 or mock transfectant cells established from SKOV-3 were immunostained with anti-CD31 and anti-αSMA. Bar, 300 μm. C, sections of tumors formed by sh-clone5 or mock transfectant cells established from DISS were immunostained with anti-CD31. Bar, 300 μm. The vascular luminal area was calculated on the basis of 5 different fields. Mean and SDs are shown ($N = 4$). *, $P < 0.01$ versus mock. D, sections of tumors formed by sh-clone5 or mock transfectant cells established from DISS were immunostained with anti-CD31 and anti-αSMA. Bar, 300 μm.

Published OnlineFirst July 23, 2012; DOI: 10.1158/1541-7786.MCR-12-0098-T

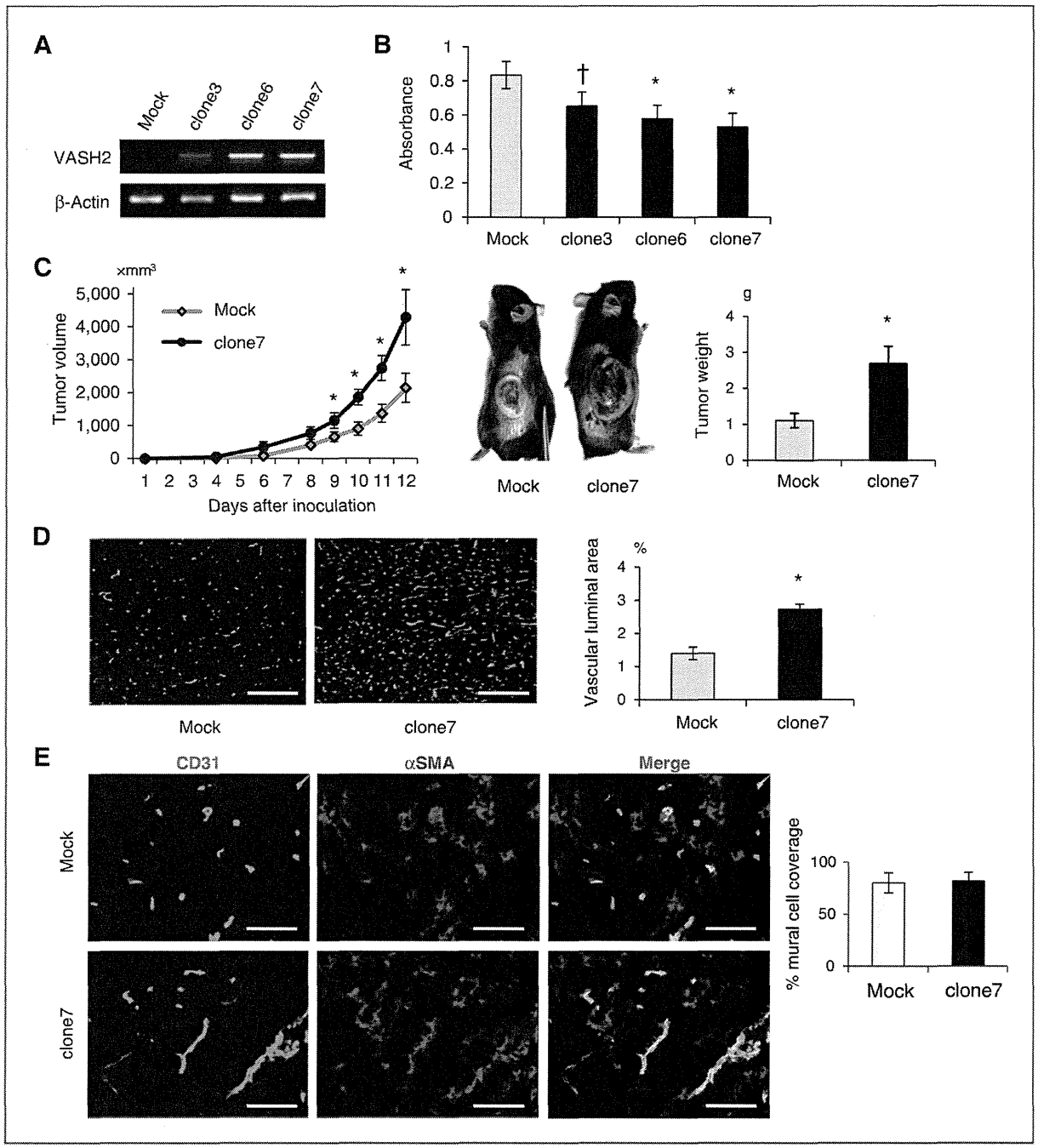

Figure 6. Stable transfection of human VASH2 gene in VASH2-negative EL-4 cells accelerated tumor growth and tumor angiogenesis *in vivo*. A, human VASH2 stable transfectants (clone3, clone6, and clone7) were established from EL-4 cells. The expression of VASH2 was determined by RT-PCR. B, proliferation of clone3, clone6, and clone7 was compared with that of the mock transfectant under the same cell culture conditions. Mean and SDs are shown ($N = 3$). *, $P < 0.01$; †, $P < 0.05$ versus mock. C, clone7 or mock cells established from EL-4 were inoculated subcutaneously into *VASH2* (−/−) mice, and the serial tumor growth was compared. Mean and SDs are shown ($N = 6$). *, $P < 0.01$ versus mock. Thirteen days after the inoculation, photographs were taken; and then the tumor weight was measured. Mean and SDs are shown ($N = 6$). *, $P < 0.01$ versus mock. D, sections of tumors formed by clone7 or mock transfectant cells established from EL-4 were immunostained with anti-CD31. Bar, 300 μm. The vascular luminal area was calculated on the basis of 5 different fields. Mean and SDs are shown ($N = 3$). *, $P < 0.01$ versus mock. E, sections of tumors from clone7 or mock transfectant cells established from EL-4 were immunostained with anti-CD31 and anti-αSMA. Bar, 100 μm.

Published OnlineFirst July 23, 2012; DOI: 10.1158/1541-7786.MCR-12-0098-T

homolog of VASH1, VASH2 may exhibit its proangiogenic effect by acting on endothelial cells as well. Here, we showed that CM from VASH2 transfectants stimulated the migration but not the proliferation of endothelial cells when compared with CM from mock transfectants (Fig. 7A). Moreover, those VASH2 transfectants as well as 2 human ovarian cancer cell lines SKOV-3 and DISS expressed SVBP (15) that plays an essential role in vasohibin secretion (Supplementary Fig. S3). These results suggest that VASH2 is secreted from cancer cells and affects on endothelial cells as a paracrine manner.

We intended to verify the mechanism of expression of VASH2 in cancer cells. We first confirmed that SKOV-3 and DISS expressed more VASH2 mRNA than HOECs (Fig. 7B). This increased expression of VASH2 in serous ovarian adenocarcinoma cells was constitutive, as no stimulus, including hypoxia, induced its expression (data not shown). To understand the mechanism of this sustained increase in VASH2 expression, we examined the involvement of microRNAs because a database for microRNA targets prediction and functional annotations (http://mirdb.org/miRDB/)/indicates VASH2 to have the highest rank as a target of miR-200b. Indeed, there are multiple binding sites of miR-200bc/429 in the 3′-untranslated region of human VASH2 mRNA (Fig. 7C). As expected, the expression of miR-200b was apparently low in SKOV-3 and DISS (Fig. 1B). Pre-miR-200b decreased the expression of VASH2 in SKOV-3 cells (Fig. 7D). Moreover, we observed an inverse correlation between VASH2 expression and miR-200b expression in human ovarian cancer tissue (Fig. 7E). These results suggest that the decreased expression of miR-200b was responsible for the upregulation of VASH2 in serous ovarian adenocarcinoma cells.

Discussion

Here, we showed for the first time that VASH2 was preferentially expressed in serous adenocarcinoma among human ovarian cancers. Moreover, specific knockdown of VASH2 from cell lines of human serous adenocarcinoma remarkably attenuated the growth of inoculated tumor cells

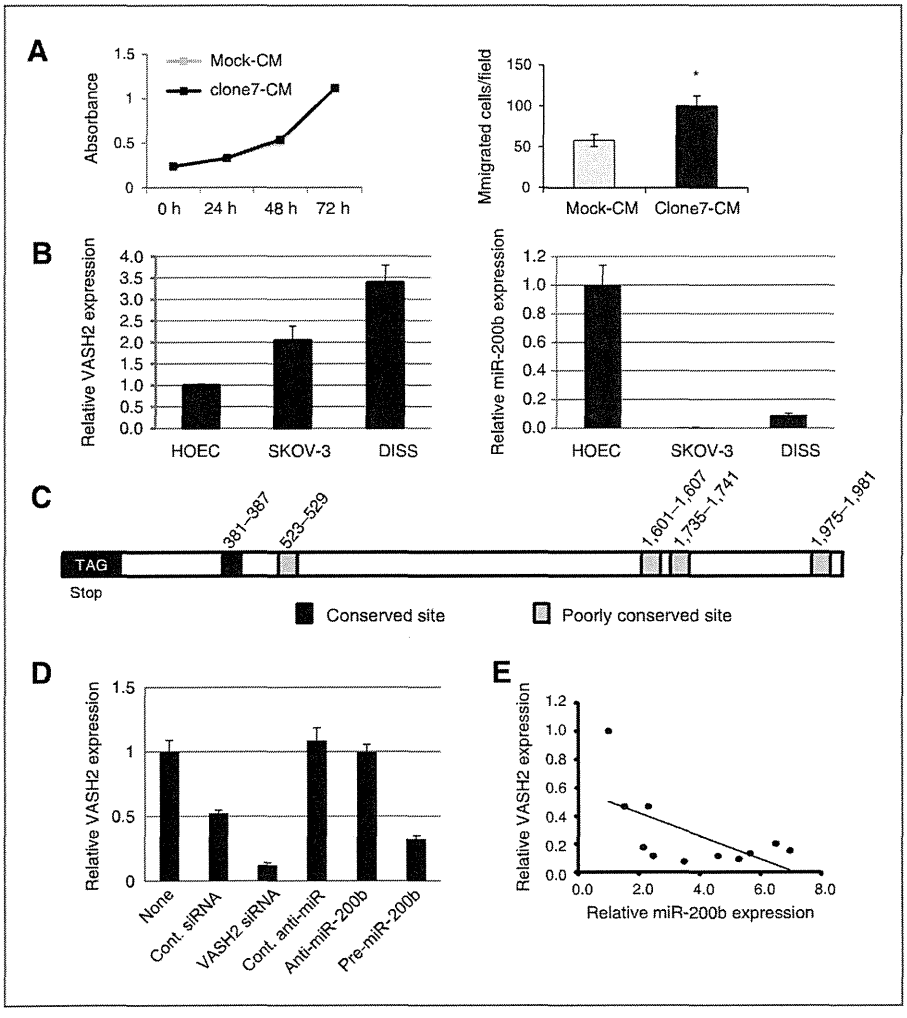

Figure 7. VASH2 stimulated migration of endothelial cells (EC) and its expression was repressed by mir-200b. A, CM from cultures of clone7 or mock transfectant cells established from EL-4 were tested for the proliferation (on the left) and migration (on the right) of ECs as described in Materials and Methods. Mean and SDs are shown ($N = 3$). *, $P < 0.01$ versus mock CM. B, expression of VASH2 and miR200b in HOEC, SKOV-3, and DISS cells was determined by conducting quantitative RT-PCR. Expression of VASH2 and miR200b in SKOV-3 and DISS was compared with that in HOECs. Means and SDs are shown ($N = 3$). C, possible binding sites of miR200bc/429 in the 3′-untranslated region of human VASH2 mRNA are shown. D, expression of VASH2 in SKOV-3 after the indicated treatment as described in Materials and Methods was determined by quantitative RT-PCR. Mean and SDs are shown ($N = 3$). Cont., control. E, total RNA was extracted from human ovarian cancer tissues, and the expression of VASH2 mRNA and miR-200b was determined by quantitative RT-PCR. $N = 11$, $R = -0.6131$, $P = 0.0448$.

Published OnlineFirst July 23, 2012; DOI: 10.1158/1541-7786.MCR-12-0098-T

and their peritoneal dissemination as well as tumor angiogenesis. In contrast, transfection of VASH2-negative tumor cells with the VASH2 gene augmented tumor angiogenesis and tumor growth when inoculated into mice. Collectively, our data suggest that VASH2 was responsible for promoting tumor angiogenesis in serous ovarian adenocarcinoma. Whereas several splicing variants of VASH2 are registered in the database, the significance and functional differences among those variants are presently obscure.

Serous adenocarcinoma is the most common histologic subtype of ovarian cancers. As mentioned earlier, because recurrence after the first-line chemotherapy is frequent, several targets have been considered for the treatment of ovarian cancers and one of them is angiogenesis (4). Antiangiogenic therapy is now approved for several cancers ranging from colon, lung, breast, and kidney; and drugs targeting VEGF signals are in clinical use (30). However, the benefit of such drugs may not last long, as patients will encounter progression of cancers because of the compensatory production of angiogenic factors other than VEGF or recruitment of bone marrow–derived angiogenic cells. Therefore, alternative targets for antiangiogenic therapy are now extensively being investigated (31). Here, we propose that VASH2 can be a candidate target for the treatment of serous adenocarcinoma in light of its stimulating effect on angiogenesis.

We have reported the proangiogenic activity of VASH2 (16), but its precise function has been unclear. Here, we showed that CM from human VASH2 transfectants stimulated the migration of endothelial cells. Ovarian cancer cells express SVBP, a secretory chaperone of vasohibins (15). These results suggest that VASH2 is secreted from the cancer cells and acts on neighboring endothelial cells to stimulate angiogenesis in a paracrine manner. VASH1 inhibits angiogenesis, whereas VASH2 stimulates it. Most plausible mechanism is that these 2 factors share a putative vasohibin receptor and one acts as an agonist whereas the other acts as an antagonist. This hypothesis is currently under investigation.

In terms of the expression of VASH2, we showed that miR-200b repressed the expression of VASH2 in ovarian cancer cells. microRNAs represent a category of small noncoding RNAs that are involved in the regulation of gene expression by translational repression and/or degradation of target mRNAs (32). The expression of VASH2 could not be induced by any of the stimuli tested (data not shown). Moreover, when murine embryonic stem cells form embryoid bodies, the expression of VASH1 is initially low but steeply induced when vessels are formed, whereas that of VASH2 is initially high in embryonic stem cells and gradually decreases during their differentiation (Abe and Sato, unpublished observations). We think that this pattern of VASH2 expression fits with the microRNA-mediated gene repression. miR-200b belongs to the miR-200 family of microRNAs. This family comprises 5 members (miR-200a, 200b, 200c, 141, and 429), and they are downregulated in cancer cells due to aberrant epigenetic gene silencing and play a critical role in the suppression of epithelial-to-mesenchymal transition (EMT) by targeting and repressing the expression of key molecules such as ZEB1 and ZEB that are involved in EMT (33). It is reported that miR-200 family members are frequently dysregulated in human ovarian cancers (34–37). In this context, it would be interesting to see whether or not VASH2 is involved in the EMT of cancer cells besides its role in angiogenesis.

In summary, VASH2 was expressed in certain ovarian cancers, and it promoted tumor growth and peritoneal dissemination of tumor cells by stimulating tumor angiogenesis. Knockdown of VASH2 significantly attenuated the tumor growth and peritoneal dissemination, which indicates that VASH2 would be a molecular target for the treatment of ovarian cancer. It is important to see whether this role of VASH2 is played in cancers from other organs.

Disclosure of Potential Conflicts of Interest

No potential conflicts of interest were disclosed.

Authors' Contributions

Conception and design: Y. Takahashi, Y. Sato
Development of methodology: Y. Takahashi, T. Moriya
Acquisition of data (provided animals, acquired and managed patients, provided facilities, etc.): Y. Takahashi, T. Koyanagi, N. Kanomata, T. Moriya
Analysis and interpretation of data (e.g., statistical analysis, biostatistics, computational analysis): Y. Takahashi, Y. Suzuki, T. Moriya
Writing, review, and/or revision of the manuscript: Y. Takahashi, T. Koyanagi, Y. Sato
Administrative, technical, or material support (i.e., reporting or organizing data, constructing databases): Y. Saga, M. Suzuki
Study supervision: Y. Sato

Grant Support

This work was supported by Grant-in-Aid for Scientific Research on Innovative Areas "Integrative Research on Cancer Microenvironment Network" (22112006) and Grants-in-Aid for Scientific Research (C) (22590821) from the Ministry of Education, Culture, Sports, Science, and Technology of Japan and a Health and Labour Sciences research grant, Third Term Comprehensive Control Research for Cancer, from the Ministry of Health, Labour, and Welfare of Japan (Y. Sato), and by the research Award to JMU Student (Y. Takahashi).

The costs of publication of this article were defrayed in part by the payment of page charges. This article must therefore be hereby marked *advertisement* in accordance with 18 U.S.C. Section 1734 solely to indicate this fact.

Received February 20, 2012; revised June 19, 2012; accepted July 7, 2012; published OnlineFirst July 23, 2012.

References

1. Bast RC Jr, Hennessy B, Mills GB. The biology of ovarian cancer: new opportunities for translation. Nat Rev Cancer 2009;9:415–28.
2. Cannistra SA. Cancer of the ovary. N Engl J Med 2004;351:2519–29.
3. Hanahan D, Weinberg RA. The hallmarks of cancer. Cell 2000;100:57–70.
4. Liu J, Matulonis UA. Anti-angiogenic agents in ovarian cancer: dawn of a new era? Curr Oncol Rep 2011;13:450–8.
5. Ferrara N. Vascular endothelial growth factor. Arterioscler Thromb Vasc Biol 2009;29:789–91.
6. Paley PJ, Staskus KA, Gebhard K, Mohanraj D, Twiggs LB, Carson LF, et al. Vascular endothelial growth factor expression in early stage ovarian carcinoma. Cancer 1997;80:98–106.
7. Duncan TJ, Al-Attar A, Rolland P, Scott IV, Deen S, Liu DT, et al. Vascular endothelial growth factor expression in ovarian cancer: a

Published OnlineFirst July 23, 2012; DOI: 10.1158/1541-7786.MCR-12-0098-T

model for targeted use of novel therapies? Clin Cancer Res 2008; 14:3030–5.
8. Byrne AT, Ross L, Holash J, Nakanishi M, Hu L, Hofmann JI, et al. Vascular endothelial growth factor-trap decreases tumor burden, inhibits ascites, and causes dramatic vascular remodeling in an ovarian cancer model. Clin Cancer Res 2003;9:5721–8.
9. Chen H, Ye D, Xie X, Chen B, Lu W. VEGF, VEGFRs expressions and activated STATs in ovarian epithelial carcinoma. Gynecol Oncol 2004;94:630–5.
10. Augustin HG, Koh GY, Thurston G, Alitalo K. Control of vascular morphogenesis and homeostasis through the angiopoietin-Tie system. Nat Rev Mol Cell Biol 2009;10:165–77.
11. Sallinen H, Heikura T, Laidinen S, Kosma VM, Heinonen S, Yla-Herttuala S, et al. Preoperative angiopoietin-2 serum levels: a marker of malignant potential in ovarian neoplasms and poor prognosis in epithelial ovarian cancer. Int J Gynecol Cancer 2010;20:1498–505.
12. Watanabe K, Hasegawa Y, Yamashita H, Shimizu K, Ding Y, Abe M, et al. Vasohibin as an endothelium-derived negative feedback regulator of angiogenesis. J Clin Invest 2004;114:898–907.
13. Shimizu K, Watanabe K, Yamashita H, Abe M, Yoshimatsu H, Ohta H, et al. Gene regulation of a novel angiogenesis inhibitor, vasohibin, in endothelial cells. Biochem Biophys Res Commun 2005;327: 700–6.
14. Shibuya T, Watanabe K, Yamashita H, Shimizu K, Miyashita H, Abe M, et al. Isolation and characterization of vasohibin-2 as a homologue of VEGF-inducible endothelium-derived angiogenesis inhibitor vasohibin. Arterioscler Thromb Vasc Biol 2006;26:1051–7.
15. Suzuki Y, Kobayashi M, Miyashita H, Ohta H, Sonoda H, Sato Y. Isolation of a small vasohibin-binding protein (SVBP) and its role in vasohibin secretion. J Cell Sci 2010;123:3094–101.
16. Kimura H, Miyashita H, Suzuki Y, Kobayashi M, Watanabe K, Sonoda H, et al. Distinctive localization and opposed roles of vasohibin-1 and vasohibin-2 in the regulation of angiogenesis. Blood 2009;113: 4810–8.
17. Yoshinaga K, Ito K, Moriya T, Nagase S, Takano T, Niikura H, et al. Expression of vasohibin as a novel endothelium-derived angiogenesis inhibitor in endometrial cancer. Cancer Sci 2008;99:914–9.
18. Hosaka T, Kimura H, Heishi T, Suzuki Y, Miyashita H, Ohta H, et al. *Vasohibin-1 expression in endothelium of tumor blood vessels regulates angiogenesis.* Am J Pathol 2009;175:430–9.
19. Tamaki K, Moriya T, Sato Y, Ishida T, Maruo Y, Yoshinaga K, et al. Vasohibin-1 in human breast carcinoma: a potential negative feedback regulator of angiogenesis. Cancer Sci 2009;100:88–94.
20. Tamaki K, Sasano H, Maruo Y, Takahashi Y, Miyashita M, Moriya T, et al. Vasohibin-1 as a potential predictor of aggressive behavior of ductal carcinoma *in situ* of the breast. Cancer Sci 2010;101: 1051–8.
21. Yoshinaga K, Ito K, Moriya T, Nagase S, Takano T, Niikura H, et al. Roles of intrinsic angiogenesis inhibitor, vasohibin, in cervical carcinomas. Cancer Sci 2011;102:446–51.
22. Yamashita H, Abe M, Watanabe K, Shimizu K, Moriya T, Sato A, et al. *Vasohibin prevents arterial neointimal formation through angiogenesis* inhibition. Biochem Biophys Res Commun 2006;345:919–25.
23. Wakusawa R, Abe T, Sato H, Yoshida M, Kunikata H, Sato Y, et al. Expression of vasohibin, an antiangiogenic factor, in human choroidal neovascular membranes. Am J Ophthalmol 2008;146:235–43.
24. Sato H, Abe T, Wakusawa R, Asai N, Kunikata H, Ohta H, et al. Vitreous levels of vasohibin-1 and vascular endothelial growth factor in patients with proliferative diabetic retinopathy. Diabetologia 2009;52:359–61.
25. Fogh J, Wright WC, Loveless JD. Absence of HeLa cell contamination in 169 cell lines derived from human tumors. J Natl Cancer Inst 1977;58:209–14.
26. Yokoyama Y, Xin B, Shigeto T, Umemoto M, Kasai-Sakamoto A, Futagami M, et al. Clofibric acid, a peroxisome proliferator-activated receptor alpha ligand, inhibits growth of human ovarian cancer. Mol Cancer Ther 2007;6:1379–86.
27. Namba K, Abe M, Saito S, Satake M, Ohmoto T, Watanabe T, et al. Indispensable role of the transcription factor PEBP2/CBF in angiogenic activity of a murine endothelial cell MSS31. Oncogene 2000;19: 106–14.
28. Yamamoto O, Hamada T, Tokui N, Sasaguri Y. Comparison of three *in vitro* assay systems used for assessing cytotoxic effect of heavy metals on cultured human keratinocytes. J UOEH 2001;23:35–44.
29. Cordero AB, Kwon Y, Hua X, Godwin AK. *In vivo* imaging and therapeutic treatments in an orthotopic mouse model of ovarian cancer. J Vis Exp 2010;42:e2125.
30. Kowanetz M, Ferrara N. Vascular endothelial growth factor signaling pathways: therapeutic perspective. Clin Cancer Res 2006;12: 5018–22.
31. Saranadasa M, Wang ES. Vascular endothelial growth factor inhibition: conflicting roles in tumor growth. Cytokine 2011;53:115–29.
32. McManus MT, Sharp PA. Gene silencing in mammals by small interfering RNAs. Nat Rev Genet 2002;3:737–47.
33. Korpal M, Kang Y. The emerging role of miR-200 family of microRNAs in epithelial-mesenchymal transition and cancer metastasis. RNA Biol 2008;5:115–19.
34. Iorio MV, Visone R, Di Leva G, Donati V, Petrocca F, Casalini P, et al. MicroRNA signatures in human ovarian cancer. Cancer Res 2007;67: 8699–707.
35. Nam EJ, Yoon H, Kim SW, Kim H, Kim YT, Kim JH, et al. MicroRNA expression profiles in serous ovarian carcinoma. Clin Cancer Res 2008;14:2690–5.
36. Yang H, Kong W, He L, Zhao JJ, O'Donnell JD, Wang J, et al. MicroRNA expression profiling in human ovarian cancer: miR-214 induces cell survival and cisplatin resistance by targeting PTEN. Cancer Res 2008;68:425–33.
37. Wyman SK, Parkin RK, Mitchell PS, Fritz BR, O'Briant K, Godwin AK, et al. Repertoire of microRNAs in epithelial ovarian cancer as determined by next generation sequencing of small RNA cDNA libraries. PLoS One 2009;4:e5311.

PLOS ONE

Angiogenesis Inhibitor Vasohibin-1 Enhances Stress Resistance of Endothelial Cells via Induction of SOD2 and SIRT1

Hiroki Miyashita[1☯], Tatsuaki Watanabe[1,2☯], Hideki Hayashi[1¤], Yasuhiro Suzuki[1], Takanobu Nakamura[1], Soichi Ito[1], Manabu Ono[1], Yasushi Hoshikawa[2], Yoshinori Okada[2], Takashi Kondo[2], Yasufumi Sato[1]*

1 Department of Vascular Biology, Institute of Development, Aging and Cancer, Tohoku University, Sendai, Japan, **2** Department of Thoracic Surgery, Institute of Development, Aging and Cancer, Tohoku University, Sendai, Japan

Abstract

Vasohibin-1 (VASH1) is isolated as an endothelial cell (EC)-produced angiogenesis inhibitor. We questioned whether VASH1 plays any role besides angiogenesis inhibition, knocked-down or overexpressed VASH1 in ECs, and examined the changes of EC property. Knock-down of VASH1 induced premature senescence of ECs, and those ECs were easily killed by cellular stresses. In contrast, overexpression of VASH1 made ECs resistant to premature senescence and cell death caused by cellular stresses. The synthesis of VASH1 was regulated by HuR-mediated post-transcriptional regulation. We sought to define the underlying mechanism. VASH1 increased the expression of (superoxide dismutase 2) SOD2, an enzyme known to quench reactive oxygen species (ROS). Simultaneously, VASH1 augmented the synthesis of sirtuin 1 (SIRT1), an anti-aging protein, which improved stress tolerance. Paraquat generates ROS and causes organ damage when administered *in vivo*. More *VASH1 (+/−)* mice died due to acute lung injury caused by paraquat. Intratracheal administration of an adenovirus vector encoding human VASH1 augmented SOD2 and SIRT1 expression in the lungs and prevented acute lung injury caused by paraquat. Thus, VASH1 is a critical factor that improves the stress tolerance of ECs via the induction of SOD2 and SIRT1.

Citation: Miyashita H, Watanabe T, Hayashi H, Suzuki Y, Nakamura T, et al. (2012) Angiogenesis Inhibitor Vasohibin-1 Enhances Stress Resistance of Endothelial Cells via Induction of SOD2 and SIRT1. PLoS ONE 7(10): e46459. doi:10.1371/journal.pone.0046459

Editor: Levon M. Khachigian, The University of New South Wales, Australia

Received April 26, 2012; **Accepted** August 30, 2012; **Published** October 8, 2012

Funding: This work was supported by grants from the programs Grant-in-Aid for Scientific Research on Innovative Areas "Integrative Research on Cancer Microenvironment Network" (22112006) and Grants-in-Aid for Scientific Research (C) [22590821] from the Ministry of Education, Culture, Sports, Science, and Technology of Japan, and by the 38th Research Grants in the Natural Sciences from the Mitsubishi Foundation. The funders had no role in study design, data collection and analysis, decision to publish, or preparation of the manuscript.

Competing Interests: The authors have declared that no competing interests exist.

* E-mail: y-sato@idac.tohoku.ac.jp

☯ These authors contributed equally to this work.

¤ Current address: Astellas Research Technology Inc., Tsukuba, Japan

Introduction

Endothelial cells (ECs) are multifunctional cells covering the entire luminal surface of all blood vessels. They form an interface between the circulating blood in the lumen and the rest of the vessel wall, and maintain vascular homeostasis. ECs control the transport of various molecules across the vascular wall, regulate immune response via the adhesion of leukocytes to the vessel wall for extravasation, manipulate vascular tonus, and prevent thrombotic events. When stimulated by angiogenic factors, ECs form neo-vessels. During the course of this process, termed angiogenesis, ECs produce molecules that control angiogenesis in an auto-regulatory manner. Endothelial tip cells produce delta-like 4, which controls the number of subsequent tips via binding to Notch1 on stalk cells [1]. We recently identified vasohibin-1 (VASH1) as an inhibitor of angiogenesis. VASH1 is expressed in ECs, whose expression is enhanced during angiogenesis, and that terminates angiogenesis as an autocrine manner [2,3].

The vascular system is one of the main target organs of aging. Age-related vascular diseases are the consequence of endothelial damage, and one of the major causes of this damage is oxidative stress [4]. When subjected to oxidative stress, cells generally exit the cell cycle and undergo premature senescence. Replicative senescence is associated with the shortening of telomeres and reduced telomerase activity, whereas premature senescence does not require those events. The oxidative stress-induced premature senescence of ECs is thought to play important roles in the pathogenesis of age-related vascular diseases, as premature senescence of ECs occurs in the vasculature of individuals who are more susceptible to develop atherosclerosis [5,6].

With respect to angiogenesis regulators, angiogenesis inhibitors generally induce EC death and vascular regression. It was recently described that one of the detectable indicators of dysfunctional senescent ECs is collagen XVIII and its C-terminal anti-angiogenic fragment, known as endostatin. Moreover, an increase in the level of endostatin exacerbates vascular damage, thus triggering a vicious cycle [7].

Here we examined the function of VASH1. As VASH1 also has anti-angiogenic activity, it may affect vascular damage. However, to our surprise, VASH1 actually enhanced the maintenance of ECs by strengthening their resistance to oxidative or serum-

starvation-induced stress. The significance of this effect and the underlying mechanism is examined in this study.

Materials and Methods

All of the animal studies were reviewed and approved by the Center for Laboratory Animal Research, Tohoku University in accordance with established standards of humane handling of research animals.

Materials

The following materials and their sources were used: α-minimal essential medium (αMEM) and Dulbecco-modified Eagle medium (DMEM) from Wako Pure Chemical Industries, Ltd. (Osaka, Japan); Superscript One-step RT-PCR with platinum Taq, Lipofectamine RNAi max, Opti-MEM I, stealth siRNAs, and 5–6-chloromethyl-2′, 7′-dichlorodihydro-fluorescein diacetate, acetyl ester (CM-H2DCFDA) from Invitrogen (Carlsbad, CA); endothelial basal medium (EBM) and endothelial cell growth supplements from Clonetics (Walkersville, MD); Isogen from Nippon Gene (Toyama, Japan); Hybond-ECL from Amersham (Buckinghamshire, UK); N-acetylcysteine (NAC), SU5416, vascular endothelial growth factor (VEGF), protein G Sepharose, anti- β-actin antibody from Sigma (St. Louis, Mo); hydrogen peroxide from Mitsubishi Chemical Corporation (Tokyo, Japan); anti-8-hydroxydeoxyguanosine (8-OHdG) antibody from Abcam (Cambridge, MA); anti-silent mating type information regulation 2 homolog 1 (SIRT1) antibody, anti-super oxide dismutase 2 (SOD2) antibody, anti-HuR antibody, ataxia teleangiectasia mutation (ATM) antibody, phospho-ATM antibody (Ser1981), anti-rabbit IgG and SIRT1 activator 3 from Santa Cruz Biotechnology (Santa Cruz, CA); and anti-light chain 3 (LC3) antibody from Medical & Biological Laboratory (Nagoya, Japan). Horseradish peroxidase (HRP)-conjugated anti-human VASH1 mAb (4E12) was described previously [2].

Cells

Human umbilical vein endothelial cells (HUVECs) and human aortic endothelial cells (HAECs) were obtained from Sanko Junyaku Industries (Tokyo, Japan) and were cultured on type I collagen-coated dishes (Iwaki, Chiba, Japan) in EBM containing endothelial cell growth supplements and 2% fetal bovine serum (FBS). All experiments using HUVECs and HAECs were performed at population doubling levels of less than 10. Normal human bronchial epithelial cells (NHBECs) were obtained from Lonza (Basel, Switzerland) and were cultured in BEGM Bullet Kit (Lonza). Mouse EC line MS1, a cell line immortalized from pancreatic ECs by SV40 large T antigen, were purchased from American Type Culture Collection (ATCC, Manassas, VA). The MS1 cells were cultured in αMEM supplemented with 10% FBS, as described previously [8].

VASH1 overexpression in HUVEC and MS1

VASH1 overexpression in human unblical vein endothelial cells (HUVECs) or in human aortic endothelial cells (HAECs) was achieved by infection with a non-proliferative adenovirus vector encoding human VASH1 (AdVASH1) at a final multiplicity of infection of 30 [2]. Alternatively, HUVECs were transiently transfected with the VASH1 expression plasmid vector [8]. VASH1 overexpressing MS1 stable clones were described previously [8].

Reverse transcriptase-polymerase chain reaction (RT-PCR)

Total RNAs were extracted and RT-PCR was performed by using a One-step RT-PCR kit (Invitrogen) according to manufacturer's instructions. Primer pairs used in this study were as follows; human VASH1 forward, 5′- ATG GAC CTG GCC AAG GAA AT-3′,and reverse, 5′- CAT CCT TCT TCC GGT CCT TG-3′;human NOX1 forward, 5′-CGT CTG CTC TCT GCT TGA AT-3′, and reverse, 5′-TGA ATC CCT AAG CCA AGG AT-3′; human NOX2 forward, 5′-GTC TGG TAT TAC CGG GTT TA-3′, and reverse, 5′-GTG CTA CTG AAT AAG GAT CAG-3′; human NOX4 forward, 5′-ATG GCT GTG TCC TGG AGG AG-3′, reverse, 5′-GAT CAT GAG GAA TAG CAC CA-3′; human SOD1 forward, 5′-AAG GAC TGA CTG AAG GCC TG-3′, and reverse, 5′-AAG CCA AAC GAC TTC CAG CG-3′; human SOD2 forward, 5′-CAG GCA GCT GGC TCC GGT TT-3′, and reverse, 5′-TGC AGT GGA TCC TGA TTT GG-3′; human SOD3 forward, 5′-ATG CTG GCG CTA CTG TGT TC-3′, and reverse, 5′-TTC CCG TTC TCC ACG CTG GC-3′; human catalase forward, 5′-ACC AGA TGC AGC ACT GGA AG-3′, and reverse, 5′-GGG GGT GTT ATT TCC AA CGA-3′; human G3PDH forward, 5′-ACC ACA GTC CAT GCC ATC AC-3′and reverse 5′- TCC ACC ACC CTG TTG CTG TA-3′.

Senescence associated β-galactosidase (SA β-gal) staining

SA beta-gal was determined by using a senescence detection kit (Abcam) according to the manufacturer's instructions. Briefly, cells were incubated overnight in freshly prepared staining solution (containing 1 μg/ml X-gal) at 37°C. The percentage of senescent cells was obtained by counting the number of blue-stained cells and the total cells per field under an inverted microscope.

Gene silencing by stealth siRNA

HUVECs or HAECs were transfected with synthetic siRNAs in Lipofectamine RNAi max containing Opti-MEM I at a final concentration of 10 nmol/L. At 12 hour post-transfection, the cell culture medium was replaced with growth medium; and the cells were then incubated for and additional 12 hours prior to use in experiments. Specific gene silencing was verified by RT-PCR and Western blot analysis. The nucleotide sequences of stealth siRNAs used in this study are as follow: for human VASH1 and its control, 5′-CAA GGA CCG GAA GAA GGA UGU UUC U-3′ and 5′-CAA CCA AGG AGA GGA GUA UUG GUC U-3′; for human HuR and its control, 5′-CGG GAU AAA GUA GCA GGA CAC AGC U -3′ and 5′-CGG AAA UGA UGG GAC CAC AAA GGC U -3′; for human SIRT1 and its control, 5′-CAG GUU GCG GGA AUC CAA AGG AUA A-3′ and 5′-CAG GCG UAA GGA CCU GGA AAU GUA A-3′; and for human SOD2 and its control, 5′-GAG GAG AAC TCG CTT CGT ATT TGT A-3 and its control, 5′-TAC TCA AAT ACG AAG CGA GTT CCU C-3′.

Immunocytochemical analysis

HUVECs on culture slides were transfected with VASH1 siRNA or control siRNA. At the desire times thereafter the cells were fixed with 4% paraformaldehyde at room temperature, and then rendered permeable with 0.1% NP-40 in PBS. Nonspecific binding sites were blocked with 1% BSA in PBS. Primary antibody reactions were performed overnight at 4°C with anti-LC-3 antibody at a dilution of 1:100. Secondary antibody reactions were performed for 1 hour at room temperature with Alexa 488-conjugated goat IgG against mouse antibody (Molecular Probes, Eugene, OR) at a 1:100 dilution with 1 μmol/L To-Pro-3 iodine

(Invitrogen). The cells were observed with a Fluoview FV4000 confocal fluorescence microscope (Olympus, Tokyo, Japan).

Western blot analysis

Western blot analysis was performed as described previously [9]. Briefly, after the poly-acrylamide gel electrophoresis and membrane transfer, the membranes were blocked for 1 hour at room temperature with Tris-HCl–buffered saline (TBS) containing 5% skim milk after the transfer, and then incubated for 1 hour at room temperature in TBS containing 0.05% Tween 20 (T-TBS), 2.5% skim milk, and one of the following antibodies: anti-human VASH1 mAb (4E12) diluted 1/500, anti-SIRT1 Ab diluted 1/500, anti-SOD2 Ab, diluted 1/500 diluted 1/500 or anti- α-actin antibody diluted 1/10,000. After the membranes had been washed 3 times with T-TBS, they incubated for 1 hour with horseradish peroxidase-conjugated protein G (Bio-Rad, Hercules, CA). They were then washed again 3 times with T-TBS, after which the blots were detected by an enhanced chemiluminescence method using an ECL Western blotting detection kit (Amersham). The results were visualized by using a LAS-4000 (Fuji Film).

Determination of SIRT1 activity

SIRT1 activity was measured by using a SIRT1 Fluorimetric Drug Discovery Kit (Biomol International, Plymouth Meeting, PA) according to the manufacturer's instructions. Briefly, cell lysates were extracted from VASH1 overexpressing or knocked-down HUVECs, and their deacetylation activity toward a peptide comprising amino acids 379–382 of human p53 (Arg-His-Lys-Lys(epsilon-acetyl)) was measured by use of a SpectraMax M2e with excitation at 360 nm and emission at 460 nm (Molecular Devices, Tokyo, Japan)

Chromatin immunoprecipitation (ChIP) assay

Total cell lysates (20 μg) derived from MS1 cells were immunoprecipitated with anti-rabbit IgG or anti-HuR antibody (5 μg) at 4°C for 3 hours. After that, 4 times-diluted Therma-Max UPA ProteinA (Magnabeat iIncorporated, Chiba, Ichihara, Japan) was added, and incubation was carried out at room temperature for 15 min. The complexes were collected according to the manufacturer's instructions. Total RNAs were extracted from the complexes, and RT-PCR analysis was performed as described above.

Trypan blue exclusion assay

Cells were incubated for 5 min in a solution of 0.2% trypan blue in PBS. More than 100 cells were counted in each field, and the percentage of non-viable cells was calculated.

Detection of cellular reactive oxygen species (ROS)

ROS was detected by using Oxiselect in vitro ROS/RNS assay kit (Cell Biolabs, San Diego, Ca) according to the manufacture's protocol. Briefly, the cell lysates (1 μg) from each treated cells were incubated with DCF-DiQxyQ for 30 min at room temperature. The fluorescence was measured by the use of SpectraMax M2e

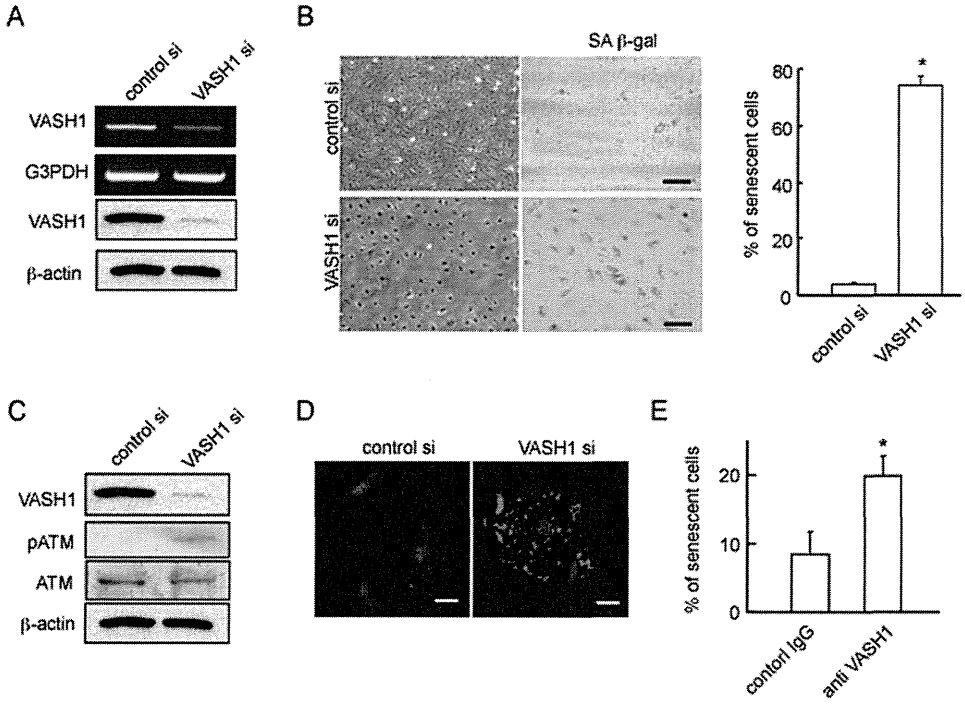

Figure 1. Knockdown of VASH1 induces premature senescence and enhances stress-induced cell death of HUVECs. (A) HUVECs were transfected with VASH1 siRNA or control siRNA. After a 24-hour incubation, RT-PCR and Western blotting for VASH1 were performed. (B) Phase-contrast photomicrographs (on the left: 48 hours after siRNA transfection) and SA beta-gal staining (on the right: 5 days after siRNA transfection) are shown. Scale bars are 250 microm. SA beta-gal-positive HUVECs were quantified, and the % senescent cells was calculated. Values are the ratio of SA beta-gal-positive cells to total cells, and are means and SDs of 3 wells. (*$P<0.01$, $N=3$). (C) HUVECs were transfected with VASH1 or control siRNA. After a 24-hour incubation, Western blotting for VASH1, ATM and p-ATM was performed. (D) HUVECs were transfected with VASH1 siRNA or control siRNA. After a 24-hour incubation, LC3 (red) was immunostained. Scale bars are 25 microm. (E) HUVECs were cultured in growth medium with 100 microM H_2O_2 including mouse IgG (control) or 10 microg/ml VASH-1 antibody (4E12) for 48 h. Trypan blue exclusion assay was performed. Blue-stained cells quantified, and the % of dead cells was calculated (*$P<0.01$, $N=3$). All the studies were repeated at least 3 times to confirm the reproducibility.

doi:10.1371/journal.pone.0046459.g001